Biosensors and Bioelectronics 142 (2019) 111530

Contents lists available at ScienceDirect

Biosensors and Bioelectronics

journal homepage: www.elsevier.com/locate/bios

Highly sensitive bioaffinity electrochemiluminescence sensors: Recent advances and future directions

Bahareh Babamiri[a,b], Delnia Bahari[a,b], Abdollah Salimi[a,b,c,*]

[a] Department of Chemistry, University of Kurdistan, 66177-15175, Sanandaj, Iran
[b] Research Center for Nanotechnology, University of Kurdistan, 66177-15175, Sanandaj, Iran
[c] Department of Chemistry, University of Western Ontario, N6A 5B7, London, Ontario, Canada

ARTICLE INFO

Keywords:
Electrochemiluminescence
Bioaffinity sensors
Aptasensor
Immunoassays
Genosensor
Cytosensor
Medical diagnostics
Nanomaterials

ABSTRACT

Electrogenerated chemiluminescence (also called electrochemiluminescence and abbreviated ECL) has attracted much attention in various fields of analysis due to the potential remarkably high sensitivity, extremely wide dynamic range and excellent controllability. Electrochemiluminescence biosensor, by taking the advantage of the selectivity of the biological recognition elements and the high sensitivity of ECL technique was applied as a powerful analytical device for ultrasensitive detection of biomolecule. In this review, we summarize the latest sensing applications of ECL bioanalysis in the field of bio affinity ECL sensors including aptasensors, immunoassays and DNA analysis, cytosensor, molecularly imprinted sensors, ECL resonance energy transfer and ratiometric biosensors and give future perspectives for new developments in ECL analytical technology. Furthermore, the results herein discussed would demonstrate that the use of nanomaterials with unique chemical and physical properties in the ECL biosensing systems is one of the most interesting research lines for the development of ultrasensitive electrochemiluminescence biosensors. In addition, ECL based sensing assays for clinical samples analysis and medical diagnostics and developing of immunosensors, aptasensors and cytosensor for this purpose is also highlighted.

1. Introduction

Designing of efficient biosensors for sensitive and selective measurement of specific biomarkers, is a significant step for the primary disease diagnosis, treatment, and management. A typical biosensing system includes of two main elements, one responsible for selective biomolecule recognition and the other for readout the corresponding signal. In bioaffinity sensors, the selective and strong binding of target biomolecules such as antibodies (Ab), aptamers or oligonucleotides, membrane receptors, with a target analyte used to produce a measurable signal (Alizadeh and salimi, 2018; Luppa et al., 2001; Hamd Qaddare and Salimi, 2017; Juzgado et al., 2017; Teymourian et al., 2017; Vo-Dinh and Cullum, 2000; Noorbakhsh and Salimi, 2011; Khezrian et al., 2013; Kavosi et al., 2015; Mansouri-Majd and Salimi, 2018; Alizadeh et al., 2017; Shahdost-fard et al., 2014). In this way, great efforts have been done for obtaining highly selective recognition and the development of new signal transduction pathways to enable quantitative detection.

Electrochemiluminescence (ECL), also referred to as electrogenerated chemiluminescence, is a kind of chemiluminescence (CL) phenomenon, whereby an ECL luminophore produced at electrode surface via an applied voltage undergo high-energy electron-transfer reactions to generate electronically excited states that luminescent signals. The ECL possesses unique superiorities over other optical methods, including photo luminescence, bio luminescence and chemiluminescence (Table 1) (Richter, 2004; Zhuo et al., 2018; Bard, 2004). First and foremost, ECL does not require an external light sources, which not only simplifies the detection apparatus but also reduces the background noises in the conventional photoluminescence sensing system (such as auto-fluorescence and scattered light), thus leading to high sensitivity. Second, compared with chemiluminescence, ECL shows distinct control toward the time and position of the light-emitting reaction because ECL emission occurs only in the diffusion layer of an electrode. The better control over the light emission position lead to enhanced selectivity, simplicity and reproducibility than CL. It should be noted that this advantage leads to the simultaneous determination of multi-analytes in the same sample by using multi-electrodes. Third, ECL is usually a nondestructive system in many cases, since the regeneration of ECL emitters can be occurred after the ECL emission. The regeneration of ECL luminophore allows them to take part in ECL

* Corresponding author. Department of Chemistry, University of Western Ontario, N6A 5B7, London, Ontario, Canada.
E-mail addresses: absalimi@uok.ac.ir, asalimi4@uwo.ca (A. Salimi).

https://doi.org/10.1016/j.bios.2019.111530
Received 14 June 2019; Received in revised form 3 July 2019; Accepted 20 July 2019
Available online 22 July 2019
0956-5663/

Table 1
Comparison of advantageous and disadvantageous of different luminescence assays.

Luminescence type	Caused by	Advantage	Disadvantage
Photoluminescence (PL)	Photoexcitation of compounds	Sensitive, Simple, Fast luminescence process,	Light source needed, High background, High phototoxicity, High photobleaching, Auto photoluminescence, Unselective photoexcitation
Bioluminescence (BL)	Luminous organisms	High sensitivity due to low background, Low cost, High-throughput imaging within living cells,	Low brightness, Long imaging time, Requirement of substrates,
Chemiluminescence (CL)	Chemical excitation of compounds	Sensitive, Linear response, Fast emission of light, No light source,	Low photon yield, Limited sensitivity, Less application,
Electrochemiluminescence (ECL)	Electrogenerated chemical excitation	Rapid and simple measurement, Wide linear range (over six order), High precision and sensitivity, Controlled reactions, Low sample volume, No light source, No background signal, Simultaneous acquisition of the current signal and the light signal	More complicated instrument, Low ECL efficiency of some new emitters, Need to development of new emitter and co-reactants,

reactions again in an excess of co-reactants. As a result, many photons are produced per measurement cycle that superior enhances the sensitivity of the technique (Hu and Xu, 2010; Fähnrich, 2001; Pyati and Richter, 2007). Finally, the ECL technique has become one of the most powerful analytical tool in design of sensor and biosensor for the trace target detection of biomolecules, clinical diagnostics, environmental and food monitoring (Miao, 2008; Marquette and Blum, 2008; Forster et al., 2009).

Over the last two decades, with the fast developing of nanomaterials based ECL assays, commercial ECL immunoassays and DNA probe assays have been widely used in the areas of clinical diagnostics due to their ability in providing sensitive, selective and rapid response (Bertoncello and Forster, 2009; Deng and Ju, 2013; Liu et al., 2015; Li et al., 2012a).

Therefore, we discuss on description and assessment of new reported applications of ECL biosensor including ECL immunoassay, multiplex ECL immunoassay, aptasensor, genosensor and MIP sensor and so on (Scheme 1). Furthermore, the application of various ECL measuring systems in biomarker analysis and applications of novel nanomaterials in ECL systems, various bioaffinity systems based on different nanomaterials was also investigated. Furthermore, ECL is powerful technique which promised for selective and sensitive determinations of analytes in clinical samples due to integrations of high affinity interactions of analytes with bioreceptors and intrinsic properties of ECL. So, ECL based sensing assays are growing importance in medical diagnostics and new applications of ECL measuring systems for clinical samples analysis in developing of immunosensors, aptasensors, genosensors and cytosensor is highlighted in this review (Table 2). However, due to the explosion of ECL application in clinical studies, this review doesn't include all of the published studies in couple past decades and we apologize to the authors of excellent work, which is unintentionally left out.

2. Analytical applications and strategies

2.1. ECL immunoassays

One of the most important development of ECL sensing is mainly focusing on clinical diagnosis, especially immunoassays. The electrochemiluminescence (ECL) immunoassay technique possesses high sensitivity and stability, fast response and simple controllability (Hu and Xu, 2010); Muzyka (2014). Thus, as an important and powerful analytical tool, ECL immunoassay has attracted much attention for ultrasensitive detection of a wide variety of analytes like virus, bacteria and protein biomarker. Over the past years, much effort has been done to improve sensitivity and develop applications of ECL immunoassays.

2.1.1. Electrochemiluminescence immunosensor for detection protein biomarker

Prostatic cancer is one of the most lethal diseases in the world that causing thousands of people to lose their lives every year. Prostate specific antigen (PSA) is a world-recognized biomarker for clinical diagnosis of prostatic cancer. Studies have shown that when the concentration of PSA rises to 2 ng mL^{-1}, it is more likely to have a prostatic cancer attack in the human immune system (He et al., 2015). Therefore, providing a method with high sensitivity and good selectivity for the quick and dynamic concentration response of PSA in human serum are urgently demanded. Fig. 1 illustrates a novel $Ru(bpy)_3^{2+}$-based electrogenerated chemiluminescence immunosensor for ultrasensitive detection of PSA utilizing palladium nanoparticle (Pd NP)-functionalized graphene-aerogel-supported Fe_3O_4 (FGA-Pd) (Yang et al., 2017c). 3D nanostructured FGA-Pd was employed as the carrier for immobilizing a large amounts of $Ru(bpy)_3^{2+}$ via electrostatic interaction to establish a brand-new ECL emitter (Ru@FGA-Pd) for improving ECL efficiency. The obtained Ru@FGA-Pd composite was applied to immobilization of the secondary antibody, which generated strong ECL signals with tripropylamine (TPrA) as a coreactant. Furthermore, gold nanoparticle (Au NP)-functionalized Fe_2O_3 nanodendrites (Au-FONDs) with good electrical conductivity and favorable biocompatibility was utilized to capture the primary antibody. This ECL strategy by virtue of the superiorities of Ru@FGA-Pd composite and of Au-FONDs show the electron-transfer rate and mass-transfer rate during the ECL emission. The fabricated sandwich-type ECL immunosensor showed a sensitive response to PSA with a low detection limit of 0.056 pg mL^{-1} (S/N = 3), the good stability (RSD of 3.15%) and favorable selectivity compared to CEA, AFP, and BSA.

The intrinsic complex luminescence mechanism involving mass transport and electron transfer (ET) dynamics of abundant radical intermediates electrogenerated on the surface of the electrode led to the relatively low ECL efficiency (Miao et al., 2002; Wang et al., 2016a)Therefore, numerous electrochemiluminescent systems was used to promote the ECL emission of luminophore through coreactant pathways (Zhou et al., 2018). Also, the long electron transfers path and great energy loss in the intermolecular ECL reaction restrict the further

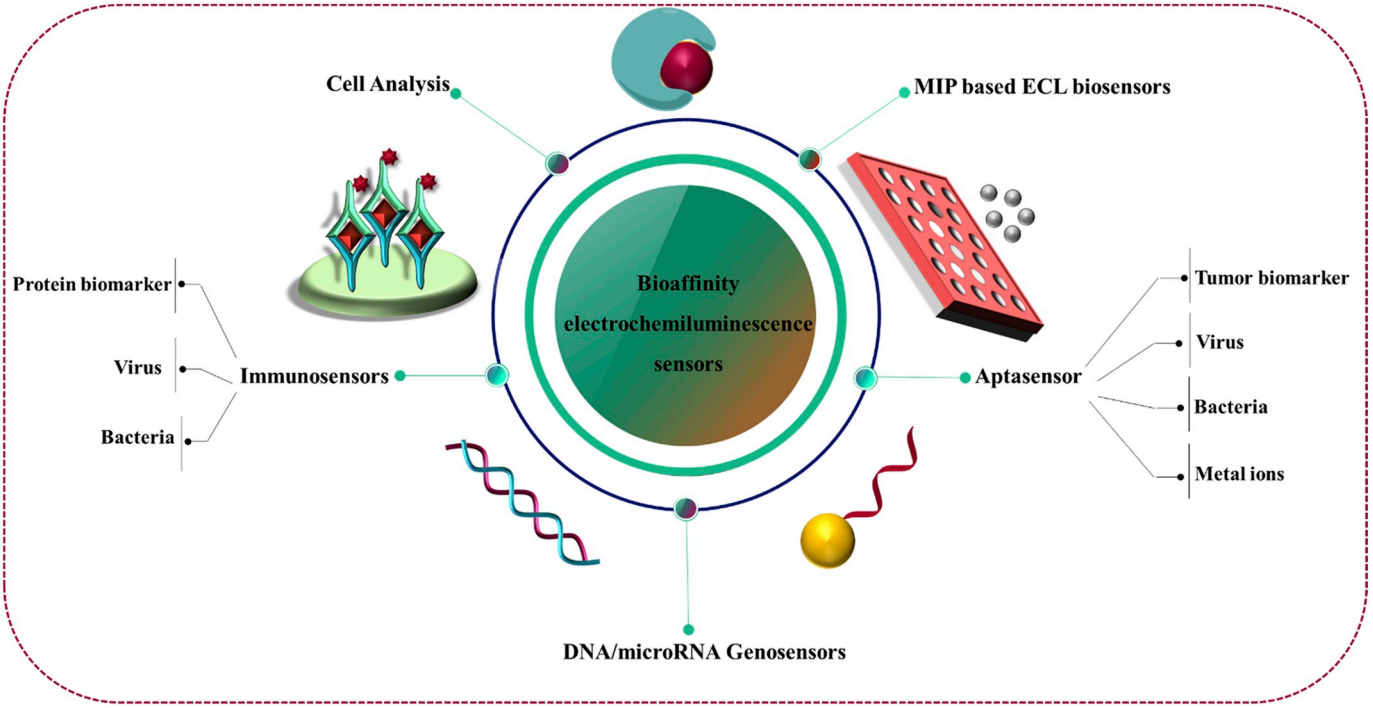

Scheme 1. Schematic presentation of applications of ECL biosensor.

development of ECL biosensors. Therefore, the self-enhanced ECL label by integrating luminophore with its coreactant in a molecular structure was designed, which exhibits excellent ECL performance due to a shorter electronic transmission distance and less energy loss.

Fig. 2 illustrates a highly sensitive electrochemiluminescence immunosensor based on the Au NCs-TAEA-Pd@CuO ternary nanostructure as highly efficient ECL label for carcinoembryonic antigen (CEA) detection (Zhou et al., 2018). In this paper, the Au nanoclusters (Au NCs) functionalized ternary nanostructure with significant electrochemiluminescence (ECL) emission, tris(3-aminoethyl) amine (TAEA) as the coreactant, and Pd@CuO nanomaterial as the coreaction accelerator was used to fabricate an ultrasensitive immunosensor for CEA detection. Herein, Pd@CuO nanomaterial was applied as the coreaction accelerator via covalent attachment so that the ECL emission of the nanostructure was up to about 40 times as compared to pure Au NCs. The proposed ECL mechanism was analogous to the widely adopted Rubpy-TPrA coreactant pathway and was listed as follows:

$$Au{\cdot}NCs - TAEA - 2e^- \rightarrow Au{\cdot}NCs^+ - TAEA^+ \quad (1)$$

$$Au{\cdot}NCs^+ - TAEA^+ \rightarrow Au{\cdot}NCs^+ - TAEA^+ + H^+ \quad (2)$$

$$\widehat{Au{\cdot}NCs^+ - TAEA^+} \xrightarrow{pd@CuO} Au{\cdot}NCs^* - TAEA \quad (3)$$

$$Au{\cdot}NCs^* - TAEA \rightarrow Au{\cdot}NCs - TAEA + hv \quad (4)$$

Through the dual self-catalysis including intramolecular coreaction acceleration from Pd@CuO to TAEA and intramolecular coreaction between TAEA and Au NCs, the Au NCs-TAEA-Pd@CuO showed excellent ECL performance, so that ECL immunosensor exhibited a wide linear range from 100 fg mL^{-1} to 100 ng mL^{-1} with a low detection limit of 16 fg mL^{-1} (S/N = 3), in the absence of any additional signal amplification assay. The proposed ECL immunosensor showed excellent stability (RSD of 2.73% for 20 cycle scans) and good specificity for CEA determination compared to different nontarget substances of α-1-fetoprotein (AFP), cardiac troponin I (cTnI), and BSA.

Among various electrochemiluminescence luminophores, N-(aminobutyl)-N-(ethylisoluminol) (ABEI), as a special analogue of luminol because of its superiorities such as chemical stability, nontoxicity, and high efficiency of luminescence, has drawn intense attention in multiple fields (Tian et al., 2011; Xie et al., 2016). Furthermore, the spatial distance between the amino and the aromatic ring of ABEI is further than luminol, that is an effective strategy to avoid the conjugated attraction effect for amino, thus considerably narrowing the space length between the electrode and the luminescent label to improve the ECL response. Since, the signal amplification strategy is a key point for the ECL biosensor fabrication, in recent years the self-enhanced ECL reagent, containing the luminophore and coreactive group in one molecular via covalently linking, has won wide attention owing to its excellent luminous efficiency (Wang et al., 2015; Swanick et al., 2012). The intramolecular reaction in the self-enhanced ECL system is an efficient strategy to the shortened electron-transfer path and reduced energy loss, which can effectively improve the ECL signal amplification. In this way, Yang and co-workers applied ABEI-PEI as a novel self-enhanced ECL reagent for the detection of β2-microglobulin (Yang et al., 2017a). In this report, ABEI − polyethylenimine (PEI) as a novel self-enhanced ECL reagent of high ECL efficiency is first prepared by cross-linking PEI with a large amount of luminophore ABEI by covalent cross-linking with the assistance of glutaraldehyde (GA). In this study, ABEI-PEI, has been chosen as a reductant and stabilizer for in situ preparation of Au@Ag nanochains (Au@AgNCs) which simultaneously realizes immobilization of numerous ECL reagents. In the following, polyacrylic acid (PAA) with a negatively charged of carboxyl group (−COO−) is pervaded on the surface of the ABEI − PEI − Au@AgNCs via electrostatic interaction and the remaining –COO− absorbing abundant Co^{2+} to form the ABEI − PEI − Au@ AgNCs − PAA/Co^{2+} complex which could introduce Co^{2+} as a catalyst, owing to the excellent catalysis of Co^{2+} to the ABEI − H_2O_2 system (Fig. 3). Finally, the obtained composites (ABEI − PEI − Au@AgNCs − PAA/Co^{2+}) was applied to immobilization of the secondary antibody. According to sandwiched immunoreactions, a sensitive ECL immunosensor is constructed to detect of β2-MG with a wide linearity from 0.01 pg mL^{-1} to 200 ng mL^{-1} and a detection limit of 3.3 fg mL^{-1}. The proposed ECL immunosensor exhibited good analytical performance and excellent stability (RSD of 3.22% for 11 cycle scans) and it was applied for β2-MG detection in human serum samples that the obtained results were found to be in acceptable agreement with the those obtained with the reference method.

Table 2
Analytical properties of different electrochemiluminescence biosensor.

Luminophore type	Sensor model	Analyte	Sensing system	Dynamic range	Detection limit	Ref
Graphene quantum dots (GQDs)	Sandwich-type immunosensor	carcinoembryonic antigen (CEA)	signal amplification strategy based on P5FIn/erGO	0.1 pg mL−1–10 ng mL−1	3.78 fg mL−1	Nie et al. (2018)
NGQDs	Sandwich-type immunosensor based ECL-RET	Prostate specific antigen (PSA)	NGQDs as the donor and Fe_3O_4@MnO_2 as the acceptor	10−5–10 ng mL-1	5 fg mL−1	Zhu et al. (2018)
CdTe	sandwich-type immunoassay	α-fetoprotein (AFP)	QDs as the signal tags and magnetic NPs as the carrier	1.0–200 ng mL-1	0.32 ng mL−1	Huang et al. (2017)
CdS:Eu	ECL-RET immunoassay	CEA	QDs as the donor and Au nanorods as acceptor	0.01 pg mL−1-1.0 ng mL−1	0.01 pg mL−1	Liu et al. (2016b)
CdSe/ZnS	sandwich-type immunoassay	CEA	TiO_2 NPs as ECL signal amplifiers and Au@PDA NPs as ECL quenchers	0.001–100 ng mL-1	0.35pg mL-1	-
$Ru(bpy)_2(phen)^{2+}$	Sandwich-type immunosensor	Carbohydrate antigen 15–3 (CA 15–3)	Self-enhanced ECL derivative (PdNC–PEI–PSRu)	0.01 U mL-1-120 U mL-1	0.003 U mL-1	Wang et al. (2014)
$Ru(bpy)_3^{2+}$	Sandwich-type immunosensor	Avian leukosis virus subgroup J (ALV-J)	pH-responsive hollow MnO_2 ($hMnO_2$) nanospheres	101.80–104.30 TCID50/mL	101.71 TCID50/mL	Liu et al. (2018a)
$Ru(bpy)_3^{2+}$	ECL immunosensor	*Escherichia coli*	$Ru(bpy)_3^{2+}$ -2-(dibutylamino)-ethanol (DBAE) system coated on ZnO NAs	200–100 000 CFU mL-1	143 CFU mL-1	Liu et al. (2018b)
ABEI	ECL immunosensor	Vibrio parahaemolyticus (VP)	signal amplification strategy based on magnetic graphene oxide	10–108 CFU mL-1	4 CFU mL-1	Sha et al. (2016)
Luminol	label-free ECL biosensor	*Staphylococcus aureus*	Based on the specific binding between Fc region of immunoglobulin G (IgG) and *S. aureus* protein A (SPA)	103–109 CFU mL-1	3.1 × 102 CFU mL-1	Yue et al. (2016)
Luminol	ECL sensor	human breast cancer cells (MCF-7)	paper-based closed bipolar electrode (BPE)	1.0 × 102–1.0 × 107cellsmL-1	40 cellsmL-1	Ge et al. (2018)
Luminol	ECL sensor	human breast cancer cells (MCF-7)	bipolar electrode mounted into 3D printed microchannel	100–700 cells	10 cells	Motaghi et al. (2018)
CdS	ECL aptasensor	CEA	Tripetalous CdS–GR nanocomposites	0.01–10.0 ng mL-1	3.8 pg mL-1	Shi et al. (2014)
ZnS–CdS	label-free ECL aptasensor	CEA	signal amplification strategy based on ZnS–CdS decorated MoS_2 nanocomposites	0.05–20.0 ng mL-1	31 pg mL−1	Wang et al. (2016b)
$[Ru(phen)_2dppz]^{2+}$	ECL aptasensor	Listeria monocytogenes	Paper-Based Bipolar Electrode Electrochemiluminescence Switch	N.R	N.R	Liu et al. (2016a)
$Ru(bpy)_3^{2+}$	ECL aptasensor	*Staphylococcus aureus*	enzyme-free branched DNA signal amplification	20 pM-100 nM	5 pM	Liu et al. (2018c)
PTC-PEI	Aptasensor ECL	Hg^{2+}	Rolling circle amplification (RCA) for signal amplification	0.1 pM-0.1 μM	33 fM	Zhao et al. (2016)
Nitrogen doped carbon dots	Aptasensor based ECL-RET	Pb^{2+}	N-CDs in situ electro-polymerized as luminophores, and Pd–Au hexoctahedrons (Pd@Au HOHs) as enhancers	1.0–1375.0 ng mL-1	0.33 ng mL-1	Xiong et al. (2016)
CdTe@CdS	Aptasensor ECL	Hg^{2+}	ECL-RET between CdTe@CdS and Au nanoparticles	20 aM-2 μM	2 aM	Babamiri et al. (2018c)
PTC-NH_2	Aptasensor ECL	Cu^{2+}	self-accelerated electrochemiluminescent nanosensor	10−13 M-1.0 × 10−7 M	3.3 × 10–14 M	Lei et al. (2018)
CdSe QDs	ECL sensor	miRNA-21	target-triggered three-way junction (3-WJ) structure combined with enzyme-powered cascade	10−14 M-10-7 M	1.5 fM	Kuang et al. (2018)
9,10-Diphenylanthracene Nanoblocks (DPA NBs)	ECL sensor	miRNA-141	Pt–Ag alloy nanoflowers as the coreaction accelerator	100 aM-1 nM	29.5 aM	Liu et al. (2018d)
$Ru(bpy)_3^{2+}$	ECL sensor	microRNA-319a	signal amplification based trigger DNA	0.5–1000 fM	0.14 fM	Wang et al. (2018)
Complex (PEI-Ru (II))	ECL sensor	miRNA-21	Quenching effect of ferrocene-labeled DNA (Fc-DNA)	0.5 fM-10 pM	0.17 fM	Peng et al. (2019)
Luminol	MIP-ECL sensor	Ni^{2+} ion	ECL sensor based on the mimetic enzyme catalytic	3.0 × 10–12 6.0 × 10−9 M	1.01 × 10−12	Yang et al. (2016)

(*continued on next page*)

Table 2 (*continued*)

Luminophore type	Sensor model	Analyte	Sensing system	Dynamic range	Detection limit	Ref
Ru $(bpy)_3^{2}$	MIP-ECL sensor	isoniazid (INH)	$Ru(bpy)_3^{2+}$-Au nanoparticles decorated multi-walled carbon nanotubes	0.1–110 mg cm-3	8 mg cm-3	Wu et al. (2012)
$Ru@SiO_2$ NPs	MIP-ECL sensor	fumonisin B1	surface-enhanced ECL based on surface plasmon resonance (LSPR) of Au NPs	0.001–100 ng mL − 1	0.35 pg mL-1	Zhang et al. (2017)
Carbon dots (C-dots)	MIP-ECL sensor	lincomycin	ECL-RET between Au-GO and C-dots	5.0×10–12–1.0×10 −9 M	1.6×10–13 M	Li et al. (2017)
EuS NCs	MIP-ECL sensor	DNA HIV	surface molecularly imprinted polymer (SMIP)	1.0 aM-10.0 nM	0.3 aM	Babamiri et al. (2018d)

Fig. 4 illustrates a 3D microfluidic origami ECL immunodevice for sensitive point-of-care testing of carcinoma antigen 125 in clinical serum samples (Wang et al., 2013). In this study, AuNPs was immobilized on the working electrode zone to enhance the rate of electron transfer and the immobilization of capture antibody (Ab_1). The luminol-AuNPs was applied as ECL luminophores and was conjugated to the signal antibodies of the ECL sandwich immunoreaction. The sandwich immunosensor shows an intense ECL emission peak with the increase of the concentration CA125 (fig). The sensor shows a linear increase in ECL intensity with increasing concentration of CA125 over the range of 0.01–100 U mL^{-1} with a low detection limit of 0.0074 U mL^{-1}. The obtained sensor has high potential applications for making point of care clinical assays in remote regions and developing countries.

2.1.2. Electrochemiluminescence immunosensor for detection of viruses

A sandwich-type electrochemiluminescence (ECL) immunosensor based on signal amplification with dendrimeric-quantum dots structures and magnetic nanoparticles was fabricated for ultrasensitive determination of HBsAg (Babamiri et al., 2018a). In order to achieve the lower detection limit and higher sensitivity, signal amplification techniques are critical needs for developing ultrasensitive electrochemiluminescence immunoassay methods. Herein, dendrimer-CdTe@CdS nanocluster and magnetic nanoparticles (MNPs) were utilized for dual signal amplification in the electrochemiluminescence immunoassay (Fig. 5). Polyamidoamine (PAMAM) dendrimers are hyper-branched and three-dimensional macromolecules with many substantial tertiary amine groups, employed as carriers for the immobilization of the QDs and the secondary antibodies (Ab_2) and the CdTe@CdS QDs were used as the luminescent labels probe to generate ECL signals. Furthermore, the functionalized magnetic nanoparticles (MNPs) with high specific surface area, were employed for HBs antibody (Ab_1) immobilization and the simplification of the separation procedures. The proposed ECL immunosensor based on the PAMAM-CdTe@CdS and magnetic nanoparticles (MNPs) showed a wide linear range from 3 fg mL^{-1} to 0.3 ng mL^{-1} with the detection limit of 0.80 fg mL^{-1} (S/N ratio of 3) for HBsAg detection and it was applied for HBsAg detection in human serum samples with satisfactory results.

2.1.3. Electrochemiluminescence biosensor for bacteria analysis

Illness and death caused by pathogenic bacteria have become one of the major threats to human health around the world. Among the different types of techniques for determination of bacteria, electrochemiluminescence assay due to its high sensitivity, wide dynamic range, stable labels and simplicity is appropriate method that are capable of detecting pathogens in near-real-time.

Vibrio parahaemolyticus (VP) is a curved, rod-shaped and gram-negative bacterium that naturally inhabits coastal and marine waters, and was frequently isolated from zooplankton, coastal fish, and shellfish and causes gastrointestinal illness in humans (Bisha et al., 2012; Drake et al., 2007). Therefore, the specific and sensitive determination of Vibrio parahaemolyticus (VP) as an important cause of sea food-associated disease is an urgently demand for sea food safety. Sha and coworkers fabricated a label free electrochemiluminescence sensor for ultrasensitive and selective detection of marine pathogenic bacterium Vibrio parahaemolyticus (VP) in sea water and sea food based on magnetic graphene oxide (nanoFe_3O_4@GO) (Sha et al., 2016). In this work, anti-VP and ABEI used as the capture device for VP and the luminophore respectively. The nano Fe_3O_4@GO with good conductivity and two-dimensional structure was employed as the carrier for immobilizing of N-(4-aminobutyl)-N-ethylisoluminol (ABEI) and VP antibody (anti-VP) which can amplify the ECL response significantly and improve the sensitivity of the proposed method (Fig. 6A). With increasing the logarithmic concentrations of VP in the range of 10–108 CFU/mL, the ECL intensity decreased and a detection limit of 5 CFU/mL for sea water and 5 CFU/g for sea food was obtained.

As a typical pathogenic bacterium, *Escherichia coli* O157:H7 is a

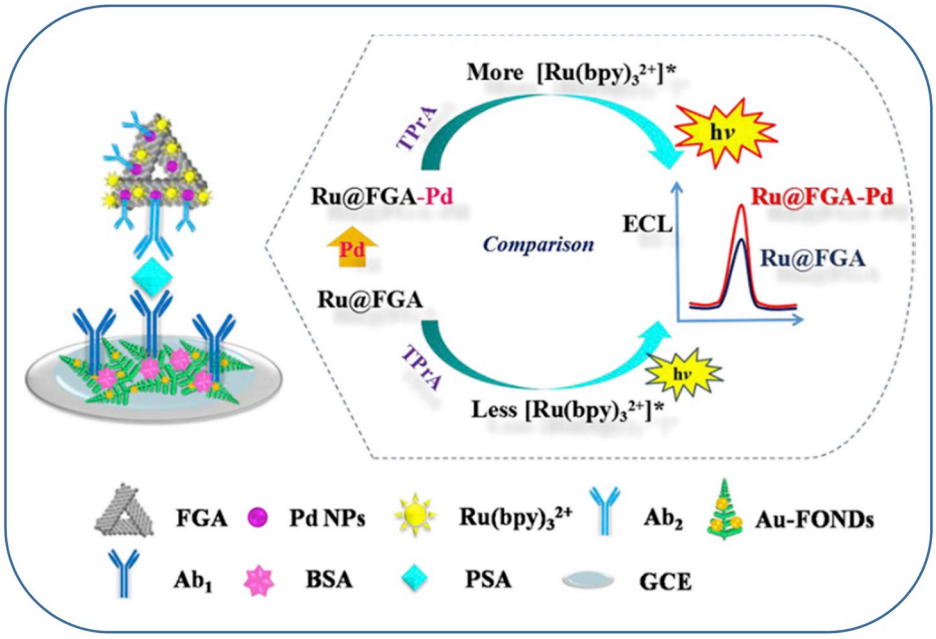

Fig. 1. Schematic representation of preparation of immunosensor array (Yang et al., 2017c).

common bacterium in both food and humans that cause serious illnesses, such as hemorrhagic colitis, hemolytic uremic syndrome and kidney failure (Jiang et al., 2016). Therefore Hao and co-workers fabricated an electrochemiluminescence sensor based on AgBr nanoparticles (NPs) anchored 3D nitrogen doped graphene hydrogel (3DNGH) nanocomposites for the detection of pathogenic bacteria *E. coli* O157:H7 (Hao et al., 2017). Three-dimensional (3D) graphene hydrogel (GH) not only maintain the excellent characteristics of graphene, but also has an exceptionally large accessible surface area even tightly packed. In this work, the ECL performance of luminol onto the surface of 3D nitrogen doped graphene hydrogel (3DNGH) for the first time were explored. Also, the ECL behavior of luminol was further amplified by using the catalysis of AgBr nanoparticles (NPs), which were also uniformly anchored throughout the surface of the 3D hierarchically porous structure. Eventually, the multifunctional nanoarchitecture was utilized as the all-solid-state ECL platform for constructing *Escherichia coli* aptasensors via glutaraldehyde as cross-linking agent between luminol/AgBr/3DNGH and amine-functionalized *E. coli* aptamer. Based on the amplified ECL signal of luminol/AgBr/3DG and the good selectivity of aptamer, a sensitive all-solid-state luminol-electrochemiluminescence *Escherichia coli* aptasensors was designed (Fig. 6B). The synthesized luminol/AgBr/3DNGH exhibited amplified ECL performances, which was about 2, 3, 8 times enhanced respectively, comparing to luminol/AgBr/3DGH, luminol/3DNGH and luminol/AgBr/2DNG. With introducing *E. coli*, the ECL intensity significantly decreased in the range from 0.5 to 500 CFU/mL with an extremely low detection limit of 0.17 CFU/mL (S/N). The excellent reproducibility (RSD of 2.31%), good specificity compared to *S. aureus*, Staphylococci and S. lactis and satisfactory results of recovery test for *E. coli* detection in real samples indicated that the suggested strategy was

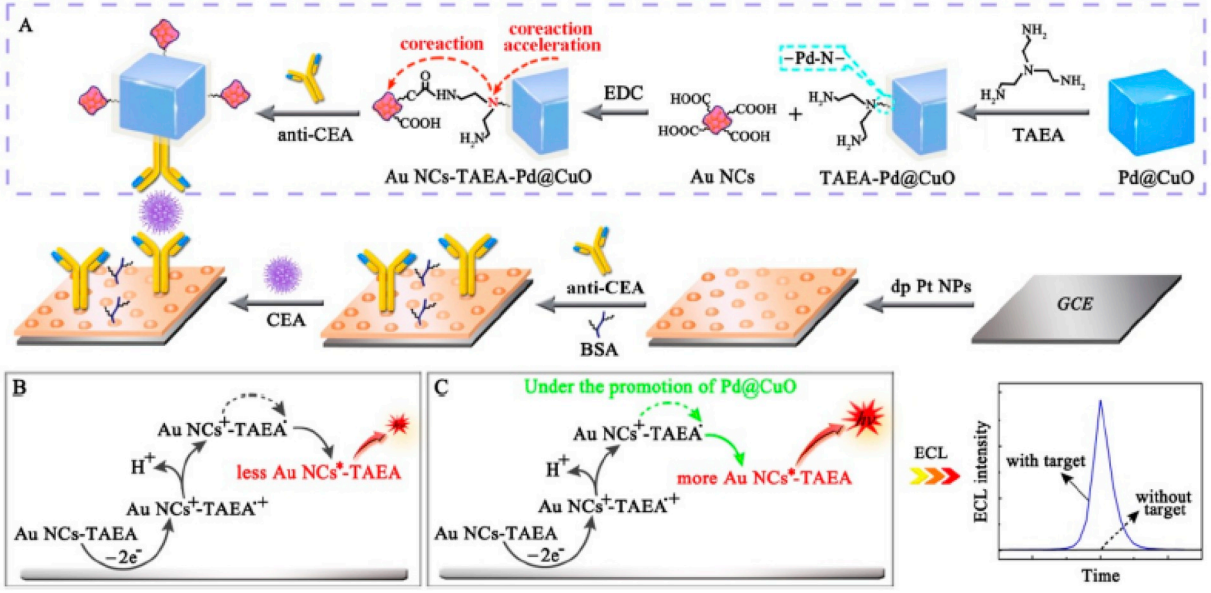

Fig. 2. (A,B) Construction of Au NCs-TAEA-Pd@CuO nanostructure and possible ECL mechanism of Only Au NCs-TAEA and Ternary ECL nanostructure with Pd@CuO as the coreaction accelerator (Zhou et al., 2018).

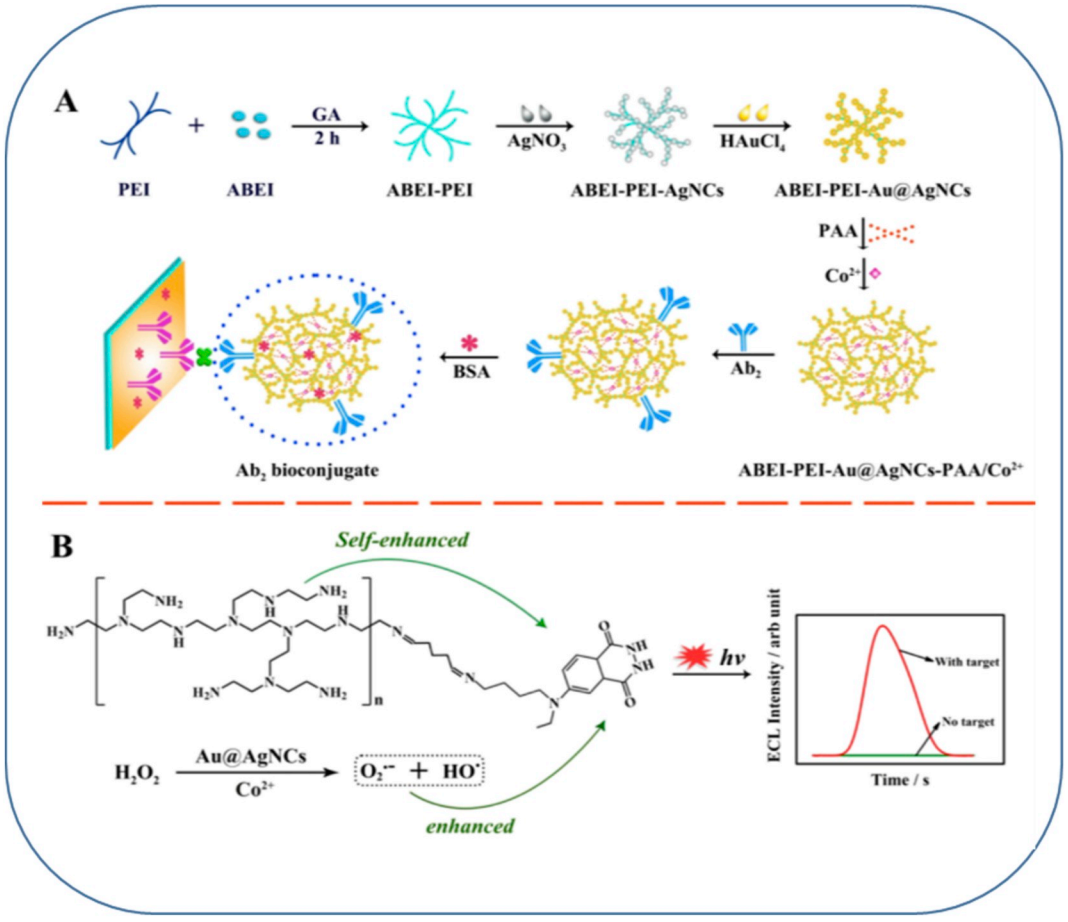

Fig. 3. Different steps for fabrication of ECL immunosensor and response mechanism (Yang et al., 2017a).

practicable for real clinical application.

2.1.4. Cell analysis

Single-cell analysis plays a significant role in the biological, medical and cellular biological function within complicated cellular environments studies. However, single-cell investigation suffers from numerous cellular processes, such as small size of a single cell, proliferation, metabolism, growth, and intra- and intercellular communication which limits the development of single-cell analysis. The conventional methods used for biological investigations reflect the average results from large cell populations, which cannot show the actual properties of an individual cell (Cannon et al., 2000; Galler et al., 2014). Thus, the development of a novel ultrasensitive assay to effectively analyze the single cell and study the individual cellular function is an urgent need. Recently, a few studies have been reported analysis of the intra- and extracellular molecules of a single cell via electrochemiluminescence (ECL) assay.

CD44, as a cell adhesion molecule expression on the cell surface, plays a substantial role in tumor biological behaviors, including prognosis, adhesion, metastasis, invasion, and survival (Li et al., 2012b; Tang et al., 2015). Since, the investigation of CD44 in a single breast cancer cell plays significant for understanding the function of CD44 in clinical studies, Qiu and co-workers fabricated a simple, ultrasensitive, and single-cell analysis platform using solid-state zinc-coadsorbed carbon quantum dot (ZnCQDs) nanocomposites as an ECL probe and graphene oxide (GO)/AuNPs as substrates of the sensing interface for the quantitative detection of breast cancer cells and assessment of the CD44 expression level on different cell-line surfaces (Qiu et al., 2017). Herein, ZnCQDs illustrated 5.5-fold enhancement of the ECL intensity, which was a contribution of a change of the surface states of CQDs leading to better conductivity of zinc ions. The ECL emission mechanism was based on electron transfer annihilation between an anionic quantum dot radical ($ZnCQDs^{\bullet -}$) and the oxidized species of the coreactant ($SO_4^{\bullet -}$) as follows:

$$ZnCQDs + ne^- \rightarrow nZnCQDs^{\bullet -} \quad (5)$$

$$S_2O_8^{2-} + e^- \rightarrow SO_4^{2-} + SO_4^{\bullet -} \quad (6)$$

$$nZnCQDs^{\bullet -} + SO_4^{\bullet -} \rightarrow nZnCQDs^* + SO_4^{2-} \quad (7)$$

$$ZnCQDs^* \rightarrow ZnCQDs + h\nu \quad (8)$$

In the following, the GO/AuNPs interface was applied to improve the ECL performance and achieve much higher stability and folic acid was further modified on the GO/AuNPs interface to capture cancer cells (Fig. 7A). Therefore, solid-state ZnCQDs nanocomposite probes were fabricated through the attachment of ZnCQDs to gold nanoparticles and the loading of magnetic beads to amplification the ECL emission that display a remarkable 120-fold enhancement of the ECL intensity. In the following, Hyaluronic acid (HA)-functionalized solid-state probes were labeled on breast cancer cells by the specific recognition of HA with CD44 on the cell surface. This strategy exhibited a good analytical performance for the analysis of MDA-MB-231 and MCF-7 single cells, and 20 single cells of these two cell lines were further analyzed in order to evaluate the cellular heterogeneity on CD44, which was first detected by ECL assay.

Some shortcomings of the traditional ECL emitters, including their biotoxicity, weak photostability and chemical stability is one of the challenges in development of ECL sensors. Upconversion nanoparticles (UCNPs) as new ECL emitter because of noteworthy advantages such as narrow emission peaks, high quantum yields, large anti-Stokes shift,

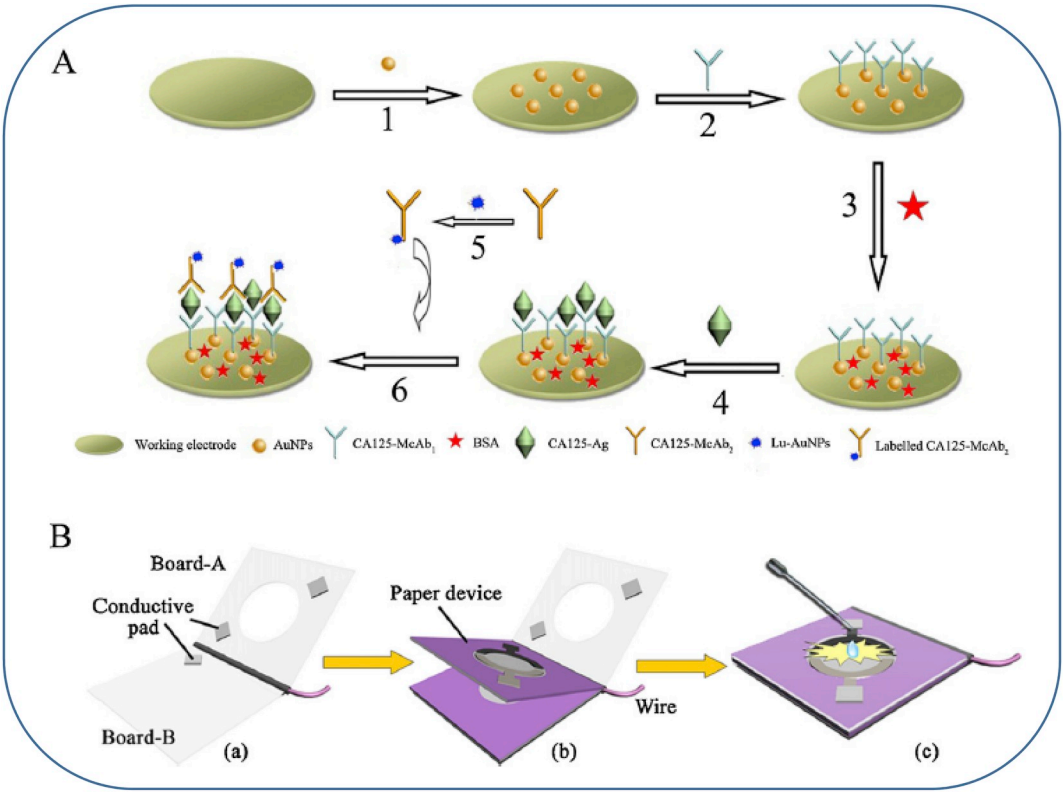

Fig. 4. (A) Schematic representation of the fabrication of the ECL immunosensor and assay procedure; (B) Schematic representation of the integration of 3D microfluidic origami immunodevice with transparent device-holder (Wang et al., 2013).

low toxicity and light stability, widely used in many fields including biological imaging, labeling, clinical therapy (Zijlmans et al., 1999; Heer et al., 2004; Zhou et al., 2012).

In this case, Zhang and co-workers proposed a novel electrochemiluminescence (ECL) cytosensor for the sensitive detection of HeLa cells (human cervical cancer cells) with the help of a signal amplification strategy by using Au–$NaYF_4$:Yb,Er nanocomposites (Zhang et al., 2018). During diagnosis process, folic acid (FA) was applied to capture folate receptor (FR) over-expressing HeLa cells. Also, HeLa cells were immobilized on the surface of the modified electrode through the interaction between folic acid and a folate receptor present on the cell surface. Furthermore, in comparison with the bare Au–$NaYF_4$:Yb,Er nanocomposites, the ECL intensity of Au–$NaYF_4$:Yb,Er nanocomposites was greatly amplified by about 4.2-fold which can be attributed to the good conductivity of gold nanoparticles (Au NPs). The ECL cytosensor illustrated high and stable ECL emission, fast response and satisfactory sensitive response to HeLa cells in a linear range of 4.25×10^2–4.25×10^5 cells per mL with a low detection limit of 326 cells per mL (Fig. 7B).

2.1.5. Multiplexing ECL-based immunoassay

Since the most markers are not specific to a particular tumor and the most cancers have more than one marker associated, so single marker immunoassay is not sufficient for the diagnosis specific cancer. Thus, the simultaneous determination of tumor markers in a single assay played a crucial role in clinical diagnosis and can dramatically improve the treatment efficiency, minimizes sample volume and handling, increases the amount of information obtainable from each sample and decreases assay cost. Multiplexing assay is customarily have been used to increase diagnostic capacity of individual testing and reduce cost by enabling multi-analyte detection in a single test run. It is known that the multiplexed immunoassay needs different labels with specific signal for each target. ECL-based assays are inherently suited to the application of multiplexing. Accordingly, ECL multiplexed immunoassay needs different labels with different potential or wavelength signals for the specific target.

Babamiri and co-workers developed the potentially-resolved electrochemiluminescence (ECL) immunoassay based on a dual signal amplification strategy by using polyamidoamine dendrimer - quantum dots (PAMAM –QDs) and PAMAM-luminol as the signal probes and Fe_3O_4–SiO_2 as a magnetic bead was designed for the simultaneous determination of two different tumor markers, alpha-fetoprotein (AFP) and carcinoembryonic antigen (CEA) (Babamiri et al., 2017). Heir in, to enhance the sensitivity of the purposed method, PAMAM dendrimers was applied as the carrier for immobilizing luminol, CdTe@CdS (QDs) and the secondary antibodies (Ab_2CEA-AFP). Also, the functionalized magnetic nanoparticles (Fe_3O_4–SiO_2 NPs) with large specific surface area and the capability of being attracted by an external magnetic field was applied as biological carriers of primary antibodies (Fig. 8A). Luminol and CdTe@CdS QDs at the presence of H_2O_2 as a co-reactant agent generate luminescence signals at +0.6 V and −1.12 V (vs Ag/AgCl), respectively (Fig. 8B). Thus, simultaneous multianalyte immunoassay could be achieved in a single run in a wide linear range from 0.25 $fgmL^{-1}$ to 20 $pgmL^{-1}$ with a very low detection limit of 0.10 $fg\,mL^{-1}$ for both analysts. The application of the immunosensor for simultaneous detection of AFP and CEA in human serum as real sample was evaluated and the obtained results were in acceptable agreement with the reference values from ELISA method. According to the obtained results this study could be creating new opportunities for the early disease diagnosis with higher efficiency.

In another study, a multiplex ultrasensitive electrochemiluminescence (ECL) immunoassay using (PAMAM-sulfanilic acid-$Ru(bpy)_3^{2+}$ -Ab_2 CA_{125}) and (PAMAM-CdTe@CdS-$Ab_{2\ CA15\text{-}3)}$ as the signal probe and Fe_3O_4@SiO_2/dendrimer as the magnetically sensor platform was fabricated for the simultaneous determination of 153 (CA 15–3) and cancer antigen 125 (CA 125) antigen cancer markers (Babamiri et al., 2018b). The CdTe@CdS-QDs and $Ru(bpy)_3^{2+}$ at the presence of tripropyl amine (TPA) as coreactant generate ECL at an

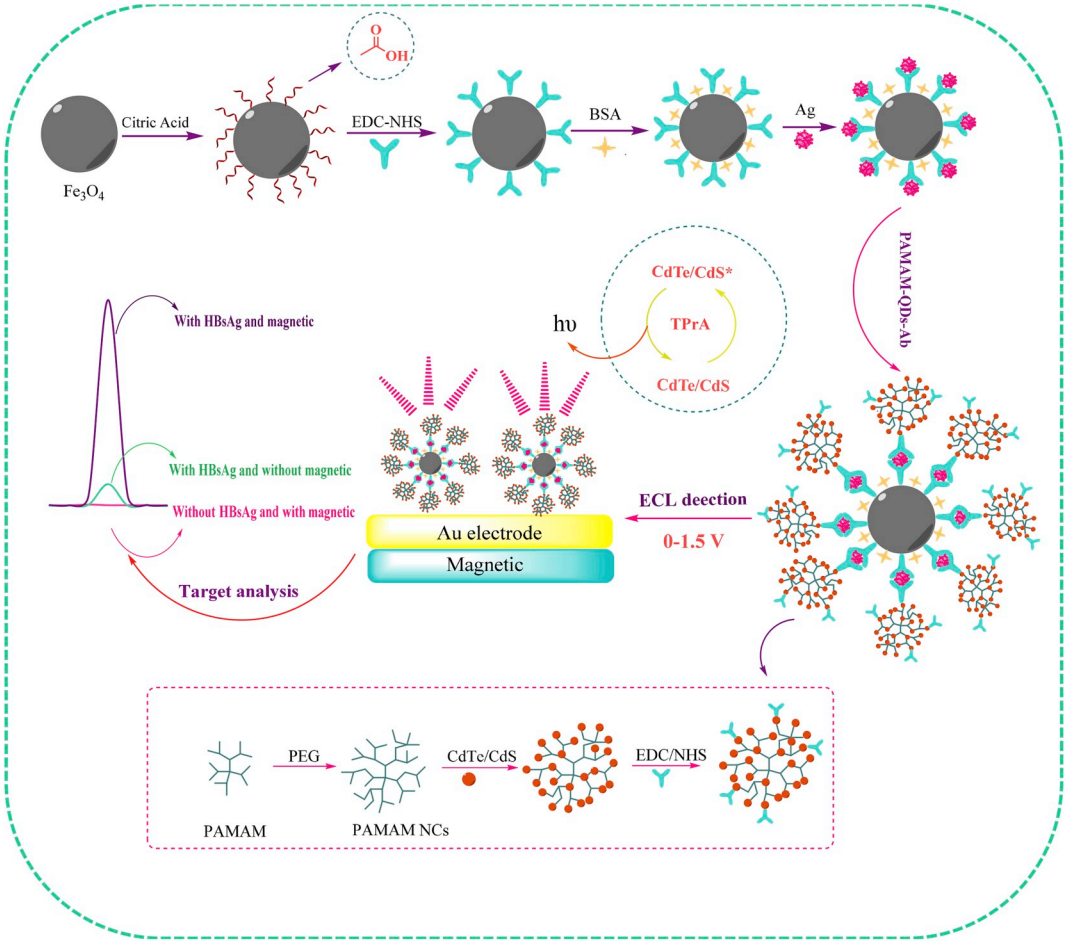

Fig. 5. Schematic illustration for the fabrication of the ECL sandwich immunoassay (Babamiri et al., 2018a).

applied voltage of +1.2 V (vs Ag/AgCl) in two different wavelengths 500 and 620 nm, respectively. Based on the proposed strategy, by employing Fe_3O_4@SiO_2-dendrimer as immunosensing platform and PAMAM as the carrier for immobilizing CdTe@CdS and $Ru(bpy)_3^{2+}$ probes, the simultaneous measurement of two tumor markers in single run carried out. As shown in Fig. 8C, at first CA 125 and CA 15–3 antibodies (Ab_1) were immobilized on Fe_3O_4@SiO_2/dendrimer. Finally, after incubation of antigens and luminescent labels, the constructed sandwich immunocomplex was assembled on the surface of ITO electrode by external magnetic forces. In cyclic voltammetric scan with tri-n-propylamine as the co-reactant agent, the amplified ECL signals at different wavelengths were obtained (Fig. 8D). With increasing concentration of CA 125 and CA 15-3 markers in the wide linear ranges of 1 μU/mL - 1 U mL^{-1} and 0.1 mU/mL-100 U/mL respectively, the ECL signal response increased. The satisfactory results from the applicability of this ECL immunoassay for real samples analysis indicated that the constructed ECL immunosensor can be used for the successfully simultaneous determination of CA 15–3 and CA 15–3 in human serum samples in clinical diagnostics.

2.2. Electrochemiluminescence aptasensor

Since, DNA probe assays have a wide range of applications in areas of medical diagnostics, environmental investigations, pharmaceutical studies, gene expression analysis and biological warfare agent detection, ECL has been used as a powerful and important analytical technique for DNA probe assays. ECL as a transducing signal for DNA probe assays is considered as a promising method to improve sensitivity and selectivity by lowering the background signal.

2.2.1. Electrochemiluminescence aptasensor for detection of cancer biomarker

Aptamers as artificially synthesized nucleic acids with benefits such as simple synthesis, high specificity and affinity, good stability, easy chemical modification widely used for highly selective detection. Over the recent years besides the traditional ECL systems such as luminol-H_2O_2 and $Ru(bpy)_3^{2+}$- tripropylamine, the new ECL luminophores based on nanomaterials including, CuS (Bansal et al., 2015), MoS_2–CdS (Shi et al., 2015), CeO_2 (Zhang et al., 2011) and CdS (An et al., 2015) have been used to developing sensitive biosensors.

Accordingly, yang and co-workers developed a signal-switchable electrochemiluminescence (ECL) aptasensor based on ferrocene-graphene sheets (Fc-GNs) for high-efficiency quenching of ECL from Au nanoparticles functionalized cadmium sulfide flower-like three dimensional (3D) assemblies (Au–CdS flowerlike 3D assemblies) for sensitive detection of prostate specific antigen (PSA) (Yang et al., 2017b). Herein, Au–CdS flower-like 3D assemblies with large surface area which was employed as luminophore, exhibiting strong and stable ECL intensity. The sensing platform was obtained by assembling captured DNA (cDNA) and hybridizing it with half of base sequence of PSA aptamer on the Au–CdS flower-like 3D assemblies the surface of modified electrode (Fig. 9). One end of the captured DNA was covalently immobilized on Au–CdS flower-like 3D assemblies modified electrode by Au–S bond and the remaining part of the non-complementary base of the aptamer could preferentially adsorb GN with the signal switched "off" state. In the following, the binding of PSA with aptamer caused desorption of aptamer from the surface of Fc-GNs and was then released from electrode surface, leading to significant signal recovery (signal switch "on" state). With the transformation of luminescence signal from

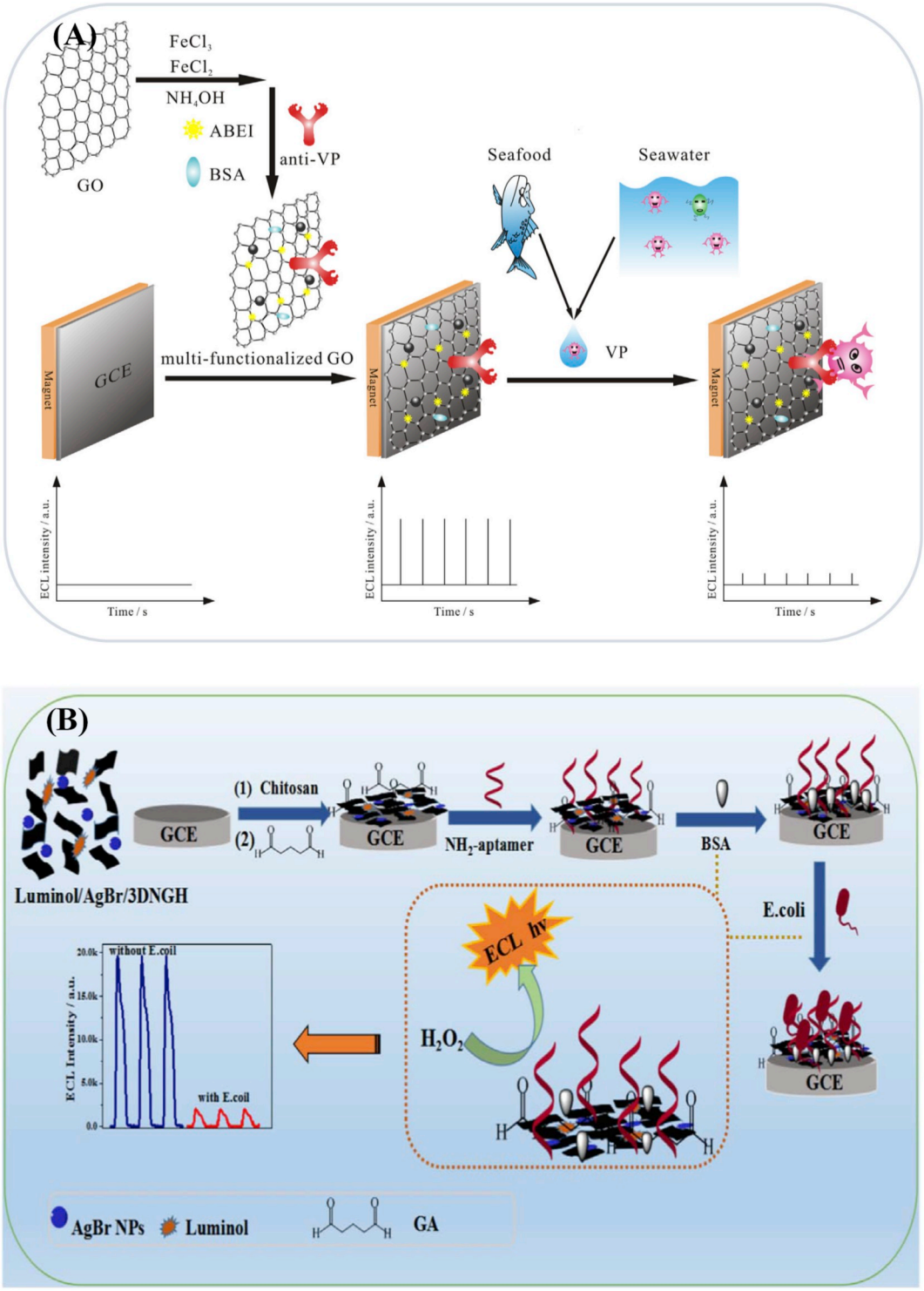

Fig. 6. (A) The schematic diagram for the preparation of multi-functionalized graphene oxide and the ECL immunosensor (Sha et al., 2016). (B) The schematic presentation for the ECL *Escherichia coli* biosensor with fabricated with luminol/AgBr/3DNGH (Hao et al., 2017).

"off" to "on", the ECL intensity significantly increased in the range of 1 pg mL^{-1} to 25 ng mL^{-1} with an extremely low detection limit of 0.38 pg mL^{-1} S/N = 3). Also, the excellent reproducibility (RSD of 2.7%), good specificity compared to interfering proteins, such as IgE, IgG and the successfully application of the determination of PSA in human serum samples with recoveries of 85.8–104.0%, suggesting great potential applications in biochemical analysis.

2.2.2. Electrochemiluminescence aptasensor for detection of metal ions

In the past few decades, the development of a simple and efficient device to identify heavy metal ions, such as Pb^{2+}, As^{3+}, Cd^{2+} and Hg^{2+}, has been one intense issue in chemical and biological domain. In this way, Zhang's group fabricated a 3D microfluidic analytical device on cellulose paper for simultaneous ECL detection of Pb^{2+} and Hg^{2+} in a single paper electrode via covalent immobilization of the corresponding oligonucleotide (aptamer). As shown in Fig. 10A, the 3D

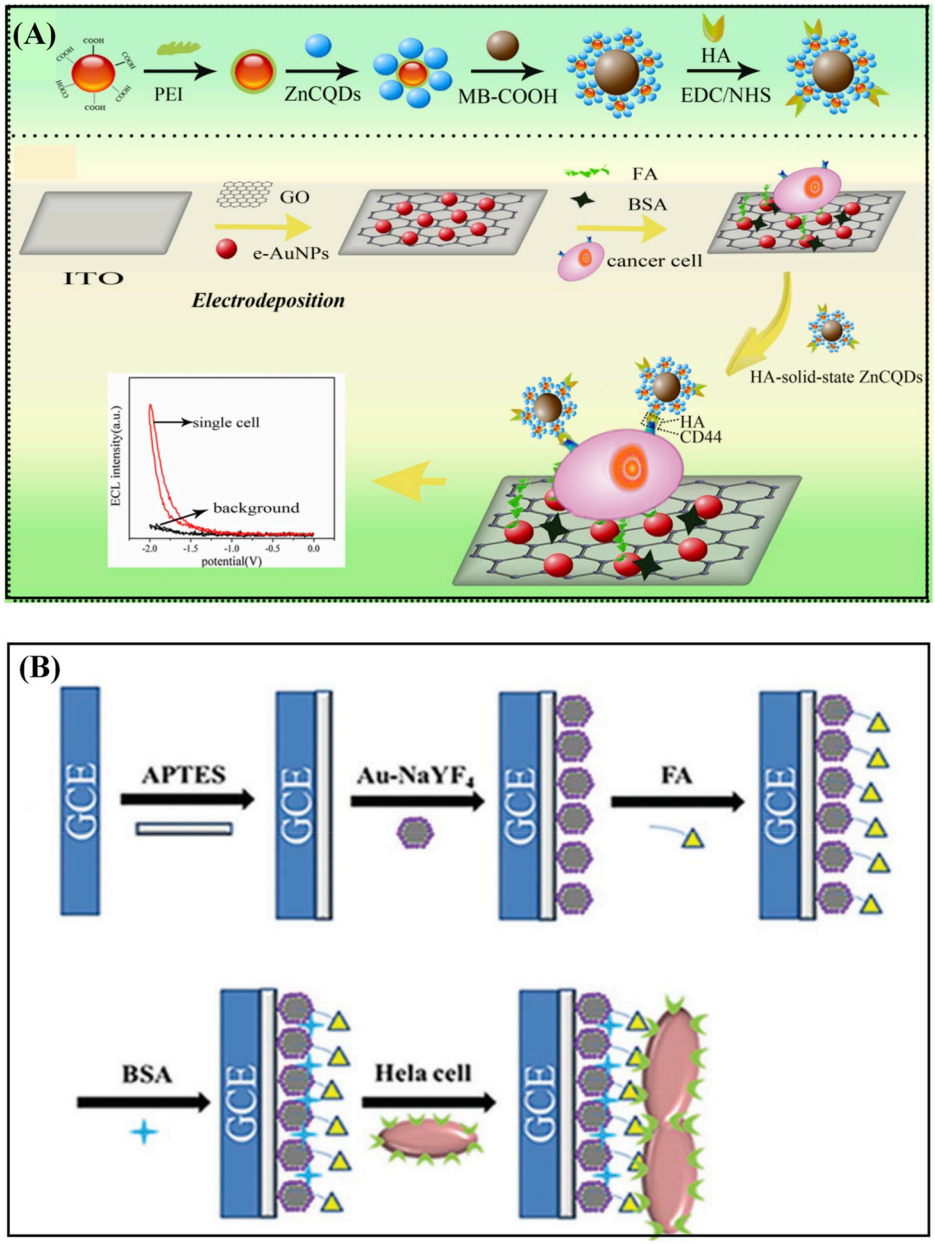

Fig. 7. (A) Preparation Process of a Multiple-Signal-Amplification Solid-State ZnCQDs Nanocomposite ECL Probe and Fabrication of the Proposed Single-Cell Analysis Platform (Qiu et al., 2017) (B) Schematic illustration of synthesizing Au–$NaYF_4$:Yb,Er nanocomposites, and schematic representation of the cytosensor based Au–$NaYF_4$:Yb,Er nanocomposites for detecting HeLa cells (Zhang et al., 2018).

paper-based ECL device was fabricated from a patterned pure cellulose paper. In the following, the aptamers are tagged with a terminal ECL label and covalently immobilized on the paper working zone of SPCWE. The $Ru(bpy)_3^{2+}$-AuNP aggregates (Ru@AuNPs) and silica nanoparticles capped with carbon nanocrystals (CNCs) (Si@CNCs) are both applied as terminal ECL labels for Hg^{2+} and Pb^{2+} determination, respectively. In the absence of metal ions, the modified aptamer chain prevents electrical contact between the ECL label and the electrode. With introducing Pb^{2+} and Hg^{2+} the immobilized aptamers fold their flexible, single-stranded chains into G-quadruplex and T–Hg–T complexes, respectively (Fig. 10B). The change in confirmation of the aptamer leads to the electrical communication of the ECL label with the electrode and producing a positive ECL signal. As illustrated in Fig. 10C, the ECL intensity of the sensor for simultaneous detection of two metal ions increased with the increasing concentration of the metal ions. The calibration plots show a good linear relationship between ECL intensity and metal ions concentration in the range of 3.0×10^{-11} to 1.0×10^{-6} M for Pb^{2+} and 5.0×10^{-10} to 1.0×10^{-6} M for Hg^{2+} with a good detection limit of 10 pM and 0.2 nM for Pb^{2+} and Hg^{2+}, respectively (Fig. 10D). Also, the low-cost POC assay was successfully applied to lake water and human serum samples and represents a simple, portable and economical method for environmental monitoring and clinical measurements.

In another study, Babamiri et al. fabricated a simple and sensitive "on-off-on" signal switching electrochemiluminescence (ECL) aptasensing assay for selective detection of Hg^{2+} (Fig. 11) (Babamiri et al., 2018c). In this electrochemiluminescence resonance energy transfer (ECL-RET) approach, Fe_3O_4@SiO_2/dendrimers/QDs showed a greatly amplified ECL signal (first signal switch "on" state). In the following, with the hybridization reaction between T-rich ssDNA (S_1) immobilized on the Fe_3O_4@SiO_2/dendrimers/QDs and AuNPs modified with complementary aptamer (AuNPs-S_2), the ECL emission of QDs

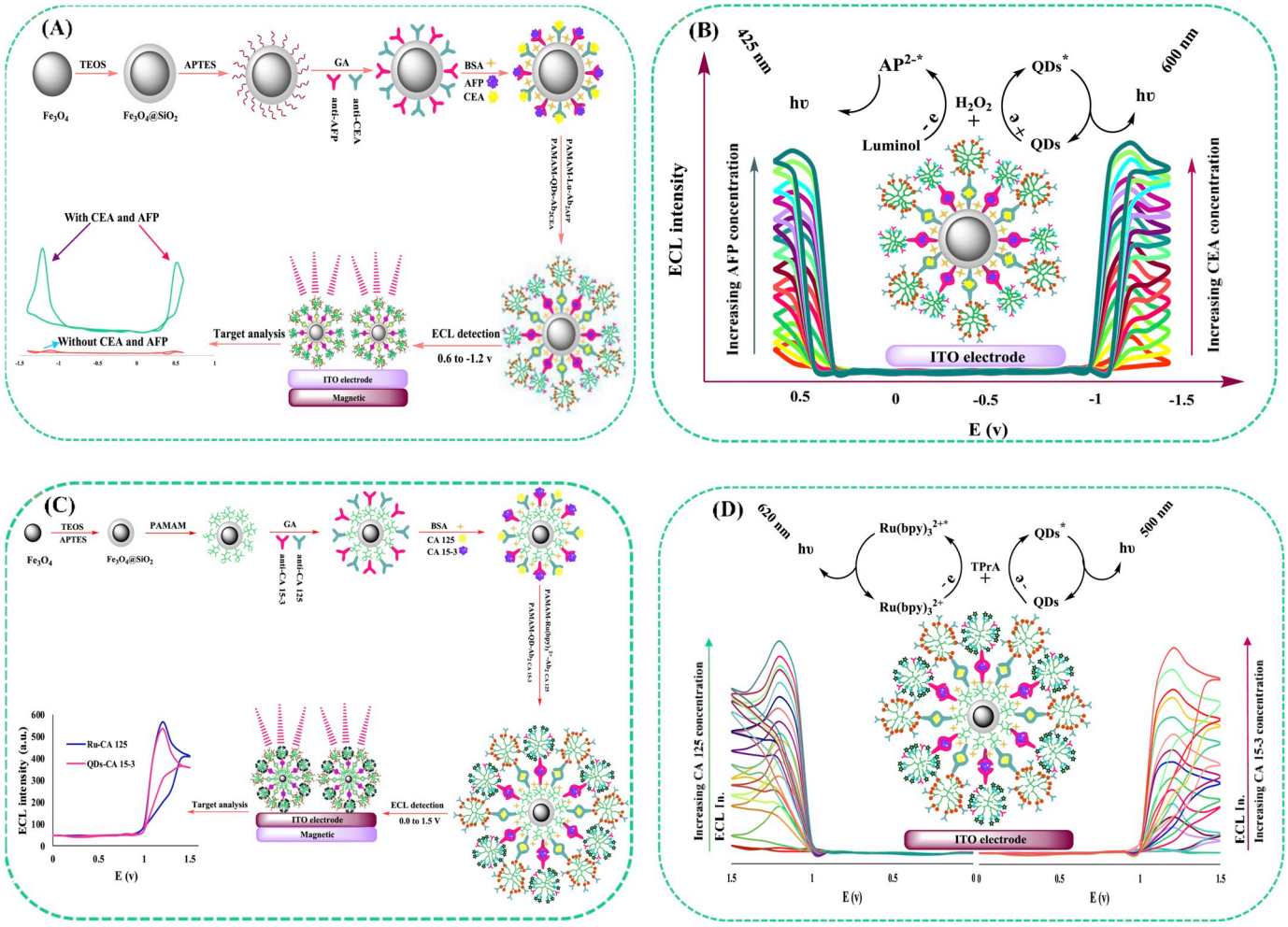

Fig. 8. (A) Schematic illustration for the fabrication of the ECL sandwich immunoassay (Babamiri et al., 2017) (B) ECL responses of the proposed immunosensor in different concentrations of CEA and AFP (C) Schematic illustration for the fabrication of the ECL sandwich immunoassay (Babamiri et al., 2018b) (D) ECL responses of the proposed immunosensor in different concentrations of CA 125 and CA 15–3.

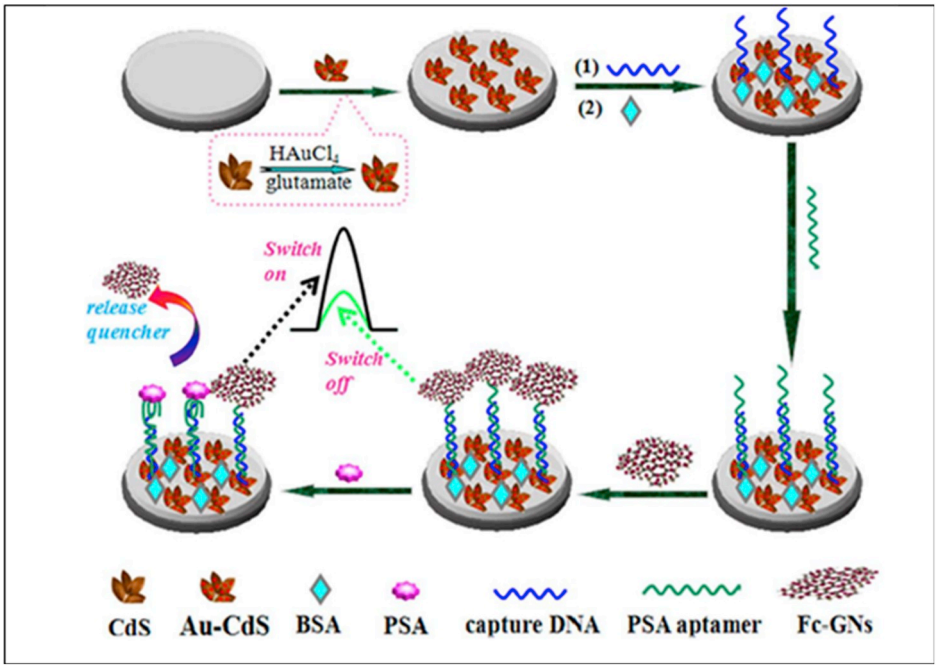

Fig. 9. Schematic illustration of the ECL biosensor for detection of PSA (Yang et al., 2017b).

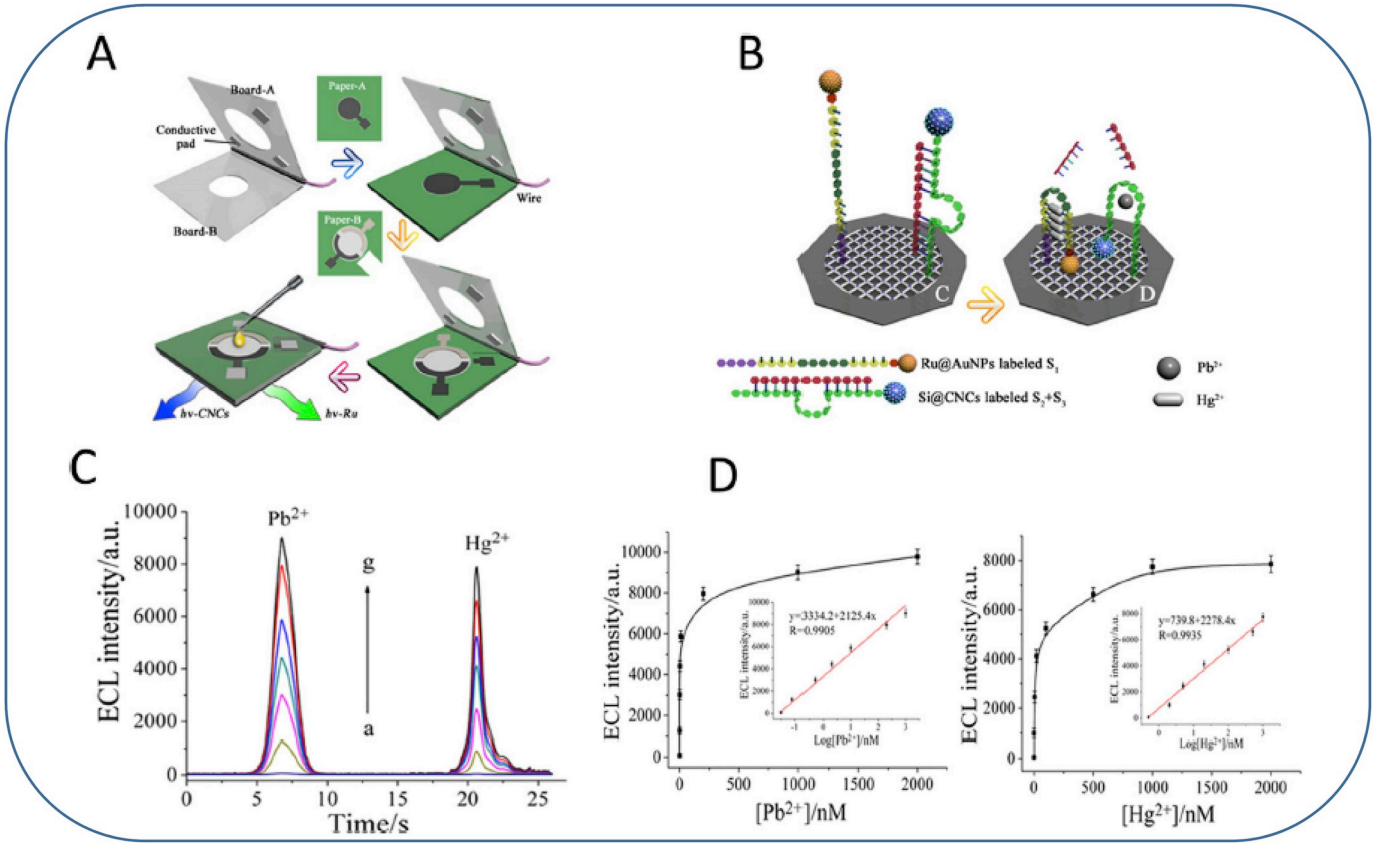

Fig. 10. Schematic representation of a 3D paper-based ECL device (A). SPCWE showing immobilized Ru@AuNP-labeled DNA strands for Hg^{2+} (Right) and Si@CNClabeled DNA strands for Pb^{2+} (Left); change in confirmation of the aptamers after capturing with Pb^{2+} and Hg^{2+} (B). ECL intensity profiles with the increasing concentration of Pb^{2+} and Hg^{2+}, in 10 mm Tris–HCl buffer (pH 7.4) (C). Calibration curves of a 3D paper-based ECL sensor for determination of Pb^{2+} and Hg^{2+} concentration. The inset shows ECL peak intensity vs. concentration of Pb^{2+} and Hg^{2+} plotted on a logarithmic scale (D) (Zhang et al., 2013).

nanocomposites was efficiently quenched (switch "off" state). Once Hg^{2+} ions were introduced into the system, aminated T-rich-ssDNA designed to capture Hg^{2+} formed a stable T-Hg^{2+}-T complex which led to the desorption of AuNPs-S_2 from double-stranded DNA (dsDNA) and the recovery of the ECL signal of QDs (second signal switch "on" state). Under optimal conditions, the designed ECL-RET aptasensor was successfully used for measurement Hg^{2+} ions with a very low detection limit of 2 aM from samples of tap waters, carp and saltwater fishes with satisfactory results.

2.3. Electrochemiluminescence genosensor for detection of microRNA

MicroRNAs (miRNAs), as a class of endogenous noncodesmall molecules (18-22 nt), play important roles as significant regulators to regulate fundamental cellular procedures via the modulation toward the expression of target genes. Research evidence has shown that miRNA is a potential class of biomarker candidate for cancer classification, early disease diagnosis, especially human cancers, neurological diseases, viral infections and diabetes (Cullen, 2004; Volinia et al., 2010). So far, many kinds of biosensors for microRNA detection have been reported (Zhang et al., 2015).

For example, as illustrated in Fig. 12A, Zhang and co-worker constructed an effective sensing platform for microRNA (miRNA) detection based on an off−on switching of a dual amplified electrochemiluminescence (ECL) biosensor based on Pb^{2+}-induced DNAzyme-assisted target recycling and rolling circle amplification (RCA). In this study, a dual amplified ECL biosensor by coupling Pb^{2+}-requiring DNAzyme-assisted target recycling amplification with Y junction has been developed for the highly sensitive miRNA detection in an off-on manner for the first time. Herein, the "switch-off" sensing platform was obtained by the quenching effect of dopamine towards a luminol/H_2O_2 system owing to the DNA hybridization reaction of the dopamine modified DNA sequence (S_1) with HP hairpin probe. At first, the primer probe was incubated with the assistant probe and the target RNA to form the Y junction structure which was cleaved with the addition of Pb^{2+} to release miRNA. The released miRNA could initiate the next recycling process, leading to the generation of abundant intermediate DNA sequences (S_2). Afterward, the treated glassy carbon electrode (GCE) was electrodeposited with $HAuCl_4$, which presented an outstanding Au nanoparticles platform to modify numerous hairpin probe (HP) through Au–S bonding. Then, dopamine (DA)-modified DNA sequence (S_1) was applied to unfold the hairpin loop of HP DNA and hybridize with HP hairpin probe, which switching off the sensing system. Due to the quenching effect of DA toward luminol, the ECL signal was reduced which indicated that the system presented the off state. Then, S_2 produced by the target recycling process was loaded onto the modified electrode to displace S_1 and served as an initiator for RCA. A numerous repeated DNA sequences coupling with hemin formed a hemin/G-quadruplex that exhibited strongly catalytic effect toward H_2O_2, which could have amplified the ECL signal to obtain the second "switch-on" state during the measurement process in the range of 1.0 fM to 100 pM. The obtained results from investigate the feasibility and capability of this method for the expression of miRNA-155 in cell lysates, including a cervical cancer cell line (HeLa), human renal cubularepithelial cell line (HK-2), normal hepatocyte cell line (L02), and human umbilical vein endothelial cell line (HUVEC) demonstrate that the proposed method provided an efficient and promising alternative tool for determining miRNA-155 in clinic analysis.

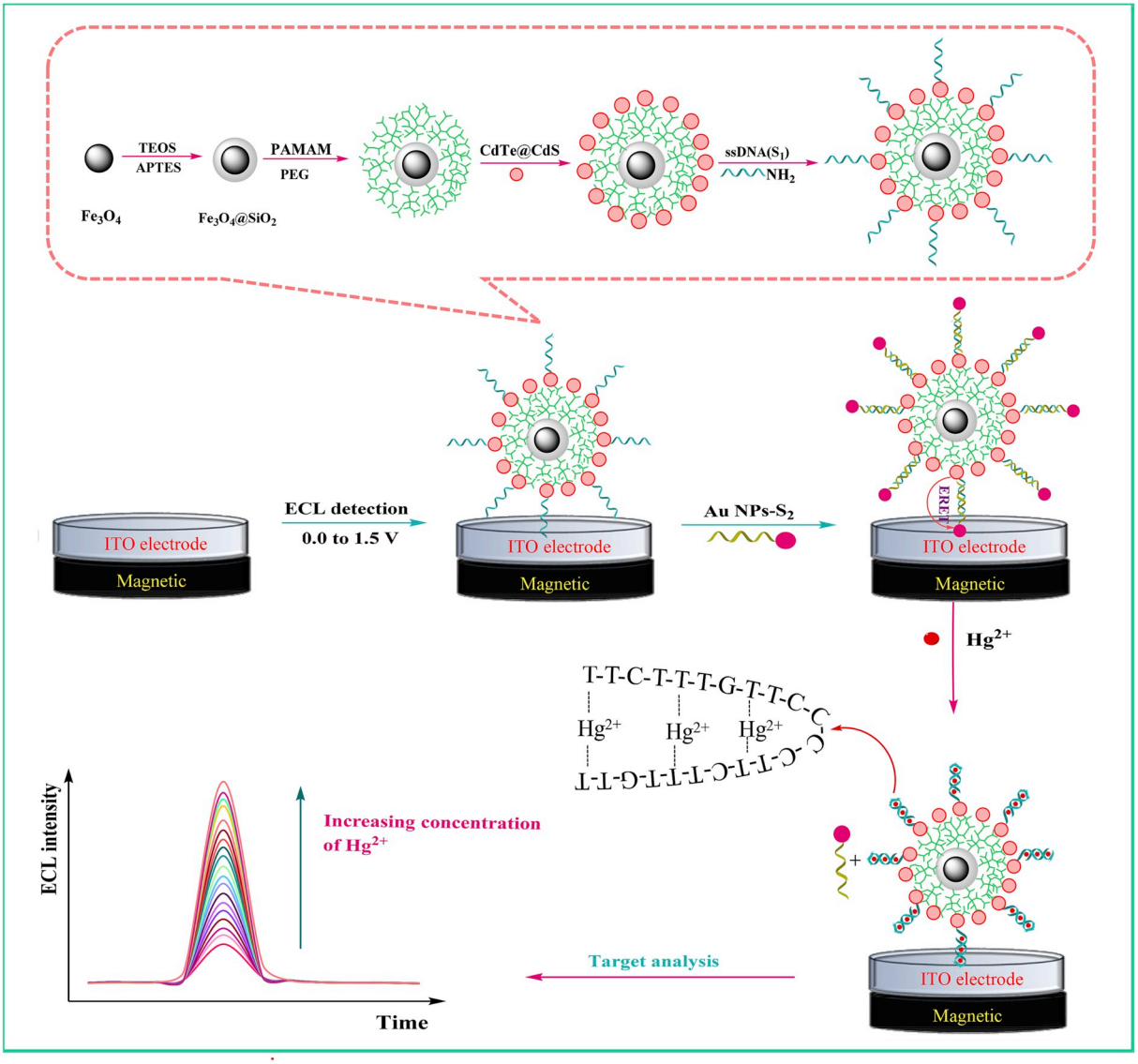

Fig. 11. Schematic representation of the ECL biosensor for Hg^{2+} detection (Babamiri et al., 2018c).

Due to insufficient information, using only one single miRNA as a biomarker may induce false positive results for diagnosis specific diseases. For example, the prostate cancer is associated with the levels of miRNA-141 and miRNA-21 that the simultaneous determination of them, can provide a more reliable measurement and showed the patterns that contribute to the diagnosis of malignancy. Thus, Shao and et al. fabricated a novel electrogenerated chemiluminescence (ECL) biosensor for the simultaneous determination of miRNA-141 and miRNA-21 based on the potential-resolved strategy (Shao et al., 2018). In this proposed biosensor, the 2D nanomaterials g-C_3N_4@AuNPs and Ru-MOF could exhibit two strong and stable ECL emissions at −1.4 V and +1.5 V respectively, which could be employed as effective potential-resolved signal tags. Herein, by immobilization of hairpin DNA_1 (HP_1) and hairpin DNA_2 (HP_2) on Fe_3O_4@Au nanocomposites, capture probes were constructed. Also, g-C_3N_4@AuNPs nanocomposites labeled by signal DNA_1 ($sDNA_1$) and ruthenium-based metal organic framework (Ru-MOF) nanosheets labeled by signal DNA_2 ($sDNA_2$) were applied as ECL emitters (Fig. 12B). Accordingly, a novel potential-resolved Faraday cage-type ECL biosensor was designed and constructed for the simultaneous detection of miRNA-141 and miRNA-21 within the linear range of 1 fM to 10 pM, with the detection limit of 0.3 fM, which could provide a feasible tool for multiple-target analysis in clinical diagnosis.

2.4. Molecularly imprinting technology-based biosensors

In recent years, molecularly imprinted polymers (MIPs) because of its superiorities such as desirable chemical and thermal stability, high adsorption capacity, effectively detection of specific molecules, excellent reusability, simplicity and low cost have been used as promising alternatives to natural receptors to developing new generation of chemical/biological sensors (Haupt, 2001; Chen et al., 2011; Wulff, 2013). On the other hand, the sensitivity and efficiency of the MIP sensors depends on the approaches of signal readout.

Among different methods such as electrochemical (Xie et al., 2010), chemiluminescence (Lin and Yamada, 2000), fluorescence (Subrahmanyam et al., 2001) and electrochemiluminescence, the electrochemiluminescent (ECL) techniques because of noteworthy advantages such as high sensitivity, low background signal, inexpensive instruments, excellent controllability and fast response is a promising analytical tool for the highly sensitive determination of the ultra-trace amounts of different targets in clinical diagnostics, environmental and biomolecule monitoring. Therefore, in this review we discuss some of new reported applications of molecularly imprinted electrochemiluminescence sensor.

As mentioned *E. coli* O157:H7 is one of the most dangerous types

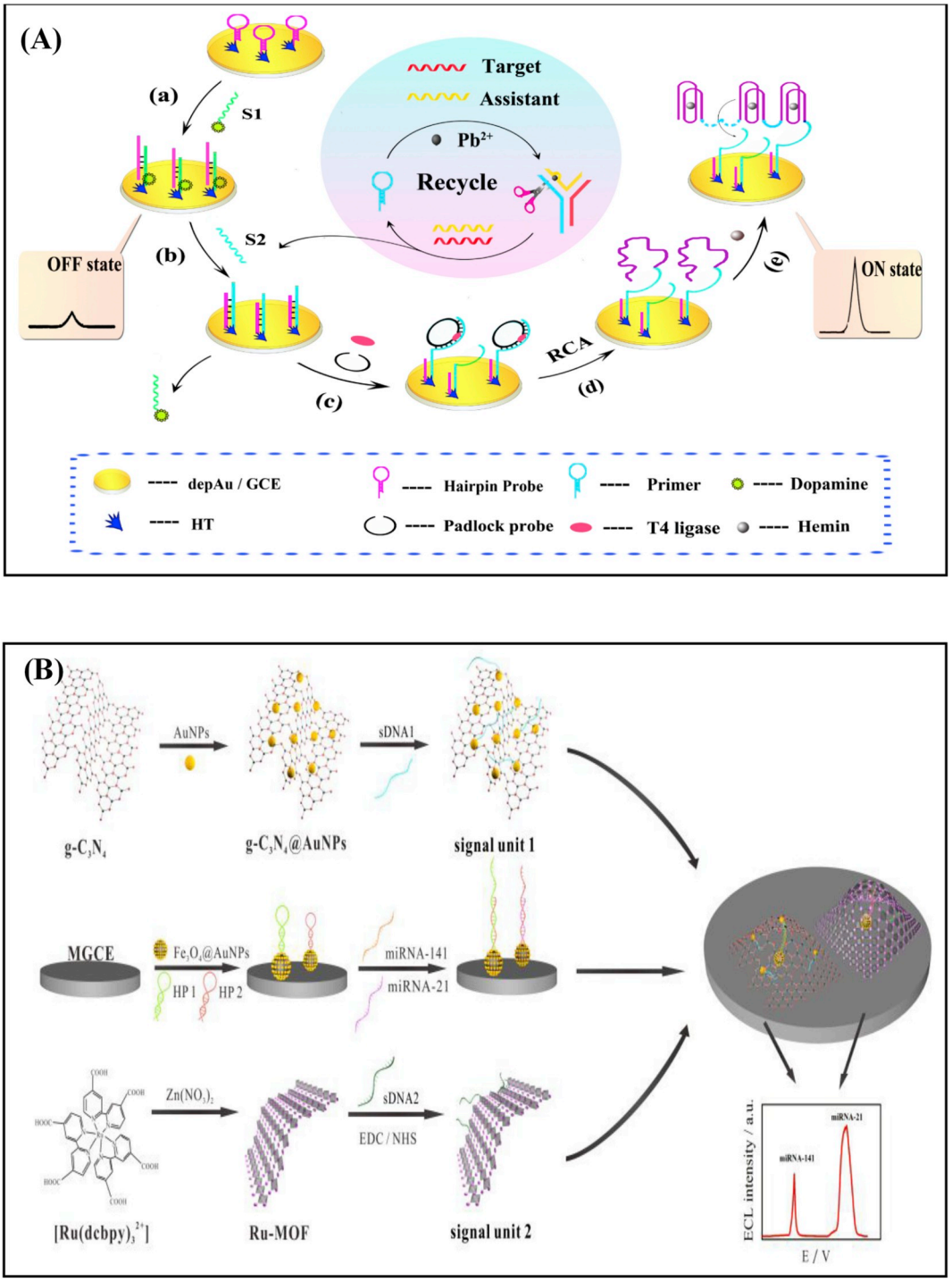

Fig. 12. (A) Schematic Diagram of Dual Amplified Assay Conducted Procedure: (a) Modification of S1, (b) Displacement of S1 by S2, (c) Incubation of T4 Ligase and Padlock Probe, (d) RCA Process, and (e) the Formation of Hemin/G-quadruplex (Zhang et al., 2015) (B) The proposed potential-resolved Faraday cage-type ECL biosensor for the determination of dual targets miRNA-141 and miRNA-21 (Shao et al., 2018).

pathogenic bacteria which can cause serious illnesses such as hemorrhagic colitis (HC) and hemolytic uremic syndrome (HUS) (Hu et al., 2016). Accordingly, Chen's group fabricated a highly electrochemiluminescence (ECL) biosensor based on polydopamine (PDA) surface imprinted polymer (SIP) and the ECL characteristics of nitrogen-doped graphene quantum dots (N-GQDs) for the quantitative detection of *Escherichia coli* (*E. coli*) O157:H7 (Chen et al., 2017). In this sensing strategy, the electropolymerization method by using the dopamine and the target bacteria was employed to form homogeneous polymer film on the electrode surface. In the co-polymerization of DA, the target bacteria were applied as template in the formation of PDA film on the electrode surface. After the *E. coli* O157:H7 template was removed, the established PDA SIP can selectively recognize and combine the target bacteria (Fig. 13A). On the other side, *E. coli* O157:H7 polyclonal antibody (pAb) was labeled with N-GQDs. Subsequently, the specific binding between the *E. coli* O157:H7 bacteria and pAb-N-GQDs on the modified GCE generated intensive ECL signal in the presence of $K_2S_2O_8$ as coreactant agent. In this work a rigid, uniform and selective

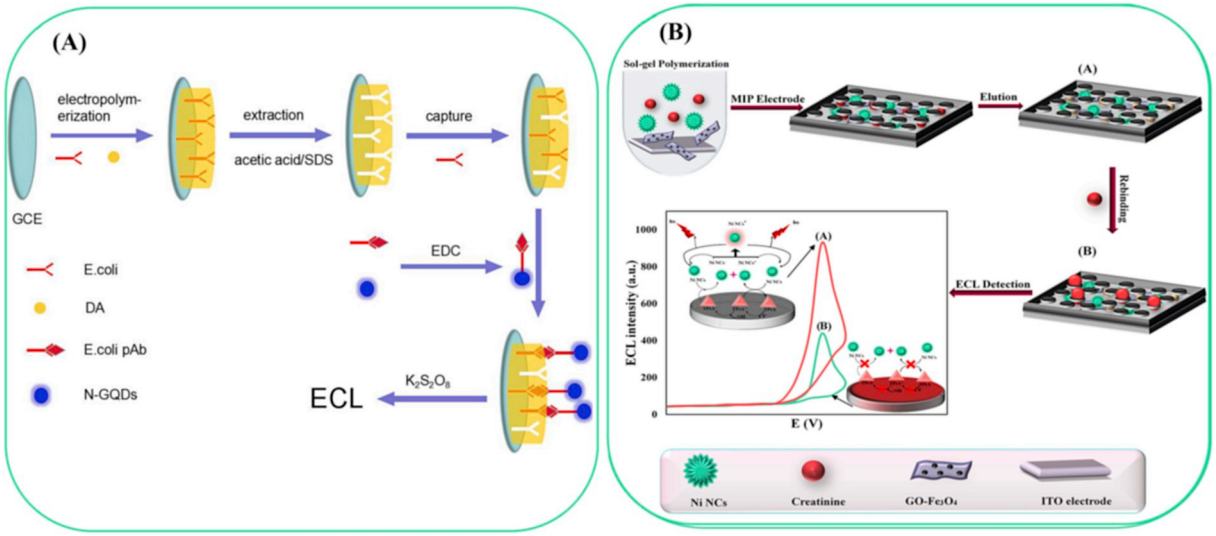

Fig. 13. (A) Schematic presentation of fabrication procedure of biosensor and detection process (Chen et al., 2017) (B) Schematic representation of the MIP-ECL assay for the detection of creatinine (Babamiri et al., 2018e).

poly dopamine (PDA) imprinted film prepared via electropolymerization method by using the ECL behavior of N-GQDs was employed for *E. coli* O157:H7 detection in the wide linear range 10^1–10^7 CFU mL^{-1} with a limit of detection (LOD) of 8 CFU mL^{-1}.

Creatinine (Cre) is the final product of the metabolism of creatine in mammals, that its concentration is less affected by the dietary changes. Therefore the sensitive and selective detection of ultra-trace amount of creatinine in blood and urine is a fairly reliable indicator in the clinical evaluation of renal function, the severity of kidney damage, muscular disorders and thyroid malfunction (Chen et al., 2006; Yamato et al., 1995). Hence, a highly sensitive and selective molecularly imprinted polymer electrochemiluminescence sensor (MIP-ECL) based on stable and water-soluble Ni nanoclusters (Ni NCs) capped with a model protein, bovine serum albumin (BSA) as a novel photoluminescent nanomaterial for highly measurement of creatinine was developed (Babamiri et al., 2018e). In this study, the uniform magnetic graphene oxide (GO-Fe_3O_4) MIP film was established on the surface of ITO electrode by sol-gel method using creatinine as template and tetraethyl orthosilicate (TEOS) as cross-linker (Fig. 12B). During the ECL process, tripropylamine (TPA) was oxidized, and Ni NCs-embedded in MIP got the energy to generate excited state Ni NCs* for light emission. (Fig. 13B). During the ECL process, tripropylamine (TPA) was oxidized, and Ni NCs-embedded in MIP got the energy to generate excited state Ni NCs* for light emission with the following equations (9)–(14):

$$TPrA - e^- \rightarrow TPrA^{\bullet +} \quad (9)$$

$$Ni\ NCs + TPrA^{\bullet +} \rightarrow Ni\ NCs^+ + TPrA \quad (10)$$

$$TPrA^{\bullet +} \rightarrow TPrA^{\bullet} + H+ \quad (11)$$

$$Ni\ NCs + TPrA^{\bullet} \rightarrow Ni\ NCs^- + Pr_2N^+CH_2{-}CH_3 \quad (12)$$

$$Ni\ NCs^+ + Ni\ NCs^- \rightarrow Ni\ NCs^* + Ni\ NCs \quad (13)$$

$$Ni\ NCs^* \rightarrow Ni\ NCs + h\nu \quad (14)$$

In the presence of creatinine, the imprinted cavities were occupied by creatinine, the ECL emission of Ni NCs on the MIP-modified electrode surface was efficiently quenched and the responses of the proposed sensing decreased with the increasing of creatinine concentration a linear range from 5 nM to 1 mM. The satisfactory results determination of creatinine in real human serum samples and urine showed that the fabricated sensor can be promised as reliable approach for creatinine measuring in clinical samples.

3. Conclusion and perspective

In conclusion, the ECL sensor is a commercially successful analytical platform with high sensitivity and excellent selectivity that is widely used for the detection of a wide range of analytes, such as biomarkers, toxins, metal ions, viruses and bacteria. The unique and attractive properties of ECL technique and the popularization of the commercial ECL instrumentation have paved the way for the development of new assays and the applications of ECL assays in clinical diagnostics, drug screening, environmental detections, biodefense, food and water safety and so on. In this review, we have the retrospect of applications of ECL bioaffinity sensing systems; including ECL immunoassay, multiplex ECL immunoassay, aptasensor, genosensor and MIP sensor and so on. A vast number of novel applications of ECL biosensors including development of new ECL light-emitting molecules and coreactants, new ECL mechanisms, investigation of molecular interaction, miniaturization of instruments, ECL imaging techniques, single molecule detection and ECL screening techniques demonstrating that the future development of electrochemiluminescence technology will continually profit from the rapid current advances. Recent developments of ECL will lead to the development of new ECL light-emitting molecules with different properties and high efficiencies and presentation of portable devices such as biomedical point-of-care devices and field instruments for use in environmental research. Furthermore, due to recent development of nanotechnology in bio sensing systems, the efficiency of ECL biosensing methods will be improved by using various nanomaterials, such as Quantum dots, Carbon dots, metal nanoclusters, graphene, etc. The nanomaterials will be used not only as luminophore but also they may be applied as quenchers in electrochemiluminescence resonance energy transfer (ECL-RET) strategies and electrochemical platform for immobilization of inorganic metal complexes (Os, Ru, Ir) and organic molecules (luminol). In addition, the miniaturization of ECL sensing methods is another area that is expected to grow rapidly with combination of microfluidic platforms or microarray technology and nanomaterials for the development of ultra-sensitive lab-on-a-chip systems for a variety of bio devices applied in clinical, food industry and environmental laboratories.

In compared to various advantageous of ECL bioaffinity sensors, there still exist several challenges such as choose the emitters and their ECL excitation potentials, intensities, wavelengths and co-reactants, the low ECL efficiency of some new emitters which could not achieve an image with high resolution for imaging systems and stability of the nanocomposites on the electrode for the development process of

ECL sensors. Furthermore, high toxicity, low efficiency or stability and none biocompatibility of emitters and co-reactants decreased the applications ranging of ECL biosensing or bioimaging systems. Also, more research is required to present new ECL emitter that are equally stable with $Ru(bpy)_3^{2+}$ but possess a higher ECL efficiency and new co-reactants that will be superior to TPrA and DBAE.

In the near future, it is expected that ECL sensing systems will be used in more creative applications with high-performance and reliable detection. Therefore, future studies will be performed toward improving ECL efficiency of luminophores and to explore the properties and ECL performance of more efficient ECL sensors. So, development of novel luminophores and various co-reactors with highly eco-friendly, low toxicity and high ECL efficiency for improving of bioimaging devices is also some future directions in this field. Development of low toxicity, creating of complete biosensing system integrated with modern telecommunications will be the next generation diagnostics systems and it seems at the future the ECL based biosensing assays will have a potential for applications to POC testing.

Declaration of interest

The authors declare that they have no known competing financial interests or personal relationships that could have appeared to influence the work reported in this paper.

CRediT authorship contribution statement

Bahareh Babamiri: Conceptualization, Writing - original draft. **Delnia Bahari:** Writing - original draft. **Abdollah Salimi:** Conceptualization, Supervision, Writing - review & editing.

Acknowledgments:

This research was supported by the Iran Nanotechnology Initiative Council (Smartphone based Sensors and Biosensors project) and the Research Offices of the University of Kurdistan, Sanandaj-Iran (grant number 4.160231). Abdollah Salimi acknowledges professor T.K. Sham (University of Western Ontario) as a host during his sabbatical and also his participation in discussions.

References

Alizade, N., Salimi, A., 2018. Electroanalysis 30, 2803–2840.
Alizadeh, N., Hallaj, R., Salimi, A., 2017. Biosens. Bioelectron. 94, 184–192.
An, B.G., Chang, Y.W., Kim, H.R., Lee, G., Kang, M.J., Park, J.K., Pyun, J.C., 2015. Sens. Actuators, B 221, 884–890.
Babamiri, B., Hallaj, R., Salimi, A., Akhtari, K., 2017. Microchim. Acta 184, 3613–3623.
Babamiri, B., Hallaj, R., Salimi, A., 2018a. Sens. Actuators, B 254, 551–560.
Babamiri, B., Hallaj, R., Salimi, A., 2018b. Biosens. Bioelectron. 99, 353–360.
Babamiri, B., Salimi, A., Hallaj, R., 2018c. Biosens. Bioelectron. 102, 328–335.
Babamiri, B., Salimi, A., Hallaj, R., 2018d. Biosens. Bioelectron. 117, 332–339.
Babamiri, B., Salimi, A., Hallaj, R., Hasanzadeh, M., 2018e. Biosens. Bioelectron. 107, 272–279.
Bansal, P., Chaudhary, G.R., Kaur, N., Mehta, S.K., 2015. RSC Adv. 5, 8205–8209.
Bard, A.J., 2004. Electrogenerated Chemiluminescence. Marcer Dekker , Inc, New York.
Bertoncello, P., Forster, R.J., 2009. Biosens. Bioelectron. 24, 3191–3200.
Bisha, B., Simonson, J., Janes, M., Bauman, K., Goodridge, L.D., 2012. Int. J. Food Sci. Technol. 47, 885–899.
Cannon Jr., D.M., Winograd, N., Ewing, A.G., 2000. Annu. Rev. Biophys. Biomol. Struct. 29, 239–263.
Chen, J., Kumar, A.S., Chung, H., Chien, S., Kuo, M., Zen, J., 2006. Sens. Actuators, B 115, 473–480.
Chen, L., Xu, S., Li, J., 2011. Chem. Soc. Rev. 40, 2922–2942.
Chen, S., Chen, X., Zhang, L., Gao, J., Ma, Q., 2017. ACS Appl. Mater. Interfaces 9, 5430–5436.
Cullen, B.R., 2004. Mol. Cell 16, 861–865.
Deng, S., Ju, H., 2013. Analyst 138, 43–61.
Drake, S.L., DePaola, A., Jaykus, L.A., 2007. Compr. Rev. Food Sci. Food Saf. 6, 120–144.
Fähnrich, K., 2001. Talanta 54, 531–559.
Forster, R.J., Bertoncello, P., Keyes, T.E., 2009. Annu. Rev. Anal. Chem. 2, 359–385.
Galler, K., Bräutigam, K., Große, C., Popp, J., Neugebauer, U., 2014. Analyst 139, 1237–1273.
Ge, S., Zhao, J., Wang, S., Lan, F., Yan, M., Yu, J., 2018. Biosens. Bioelectron. 102, 411–417.
Hamd Qaddare, S., Salimi, A., 2017. Biosens. Bioelectron. 89, 773–780.
Hao, N., Zhang, X., Zhou, Z., Hua, R., Zhang, Y., Liu, Q., Qian, J., Li, H., Wang, K., 2017. Biosens. Bioelectron. 97, 377–383.
Haupt, K., 2001. Analyst 126, 747–756.
He, Y., Xie, S., Yang, X., Yuan, R., Chai, Y., 2015. ACS Appl. Mater. Interfaces 7, 13360–13366.
Heer, S., Kömpe, K., Güdel, H.U., Haase, M., 2004. Adv. Mater. 16, 2102–2105.
Hu, L., Xu, G., 2010. Chem. Soc. Rev. 39, 3275–3304.
Hu, R.R., Yin, Z.Z., Zeng, Y.B., Zhang, J., Liu, H.Q., Shao, Y., Ren, S.B., Li, L., 2016. Biosens. Bioelectron. 78, 31–36.
Huang, Z.J., Han, W.D., Wu, Y.H., Hu, X.G., Yuan, Y.N., Chen, W., Peng, H.P., Liu, A.L., Lin, X.-H., 2017. J. Electroanal. Chem. 785, 8–13.
Jiang, T., Song, Y., Wei, T., Li, H., Du, D., Zhu, M.J., Lin, Y., 2016. Biosens. Bioelectron. 77, 687–694.
Juzgado, A., Soldà, A., Ostric, A., Criado, A., Valenti, G., Rapino, S., Conti, G., Fracasso, G., Paolucci, F., Prato, M., 2017. J. Mater. Chem. B 5, 6681–6687.
Kavosi, B., Salimi, A., Hallaj, R., Moradi, F., 2015. Biosens. Bioelectron. 74, 915–923.
Khezrian, S., Salimi, A., Teymourian, H., Hallaj, R., 2013. Biosens. Bioelectron. 43, 218–225.
Kuang, Q., Li, C., Qiu, Z., Jie, G., Niu, S., Huang, T., 2018. Sens. Actuators, B 274, 116–122.
Lei, Y.M., Xiao, B.Q., Liang, W.B., Chai, Y.Q., Yuan, R., Zhuo, Y., 2018. Biosens. Bioelectron. 109, 109–115.
Li, J., Guo, S., Wang, E., 2012a. RSC Adv. 2, 3579–3586.
Li, J., Zha, X.M., Wang, R., Li, X.D., Xu, B., Xu, Y.J., Yin, Y.M., 2012b. Biomed. Pharmacother. 66, 144–150.
Li, S., Liu, C., Yin, G., Zhang, Q., Luo, J., Wu, N., 2017. Biosens. Bioelectron. 91, 687–691.
Lin, J., Yamada, M., 2000. Anal. Chem. 72, 1148–1155.
Liu, Z., Qi, W., Xu, G., 2015. Chem. Soc. Rev. 44, 3117–3142.
Liu, H., Zhou, X., Liu, W., Yang, X., Xing, D., 2016a. Anal. Chem. 88, 10191–10197.
Liu, J., Cui, M., Zhou, H., Zhang, S., 2016b. Sci. Rep. 6, 30577.
Liu, C., Hou, J., Waterhouse, G.I.N., Cui, L., Dong, J., Ai, S., 2018a. Biosens. Bioelectron. 118, 167–173.
Liu, D., Li, T., Huang, W., Ma, Z., Zhang, W., Zhang, R., Yan, H., Yang, B., Liu, S., 2018b. Nanotechnology 30, 25501.
Liu, J.L., Tang, Z.L., Zhang, J.Q., Chai, Y.Q., Zhuo, Y., Yuan, R., 2018c. Anal. Chem. 90, 5298–5305.
Liu, Y., Wei, Y., Cao, Y., Zhu, D., Yu, Y., Guo, M., 2018d. Biosens. Bioelectron. 117, 830–837.
Luppa, P.B., Sokoll, L.J., Chan, D.W., 2001. Clin. Chim. Acta 314, 1–26.
Mansouri Majd, S., Salimi, A., 2018. Anal. Chim. Acta 1000, 273–282.
Marquette, C.A., Blum, L.J.L.J., 2008. Anal. Bioanal. Chem. 390, 155–168.
Miao, W., 2008. Chem. Rev. 108, 2506–2553.
Miao, W., Choi, J., Bard, A.J., 2002. J. Am. Chem. Soc. 124, 14478–14485.
Motaghi, H., Ziyaee, S., Mehrgardi, M.A., Kajani, A.A., Bordbar, A.K., 2018. Biosens. Bioelectron. 118, 217–223.
Muzyka, K., 2014. Biosens. Bioelectron. 54, 393–407.
Nie, G., Wang, Y., Tang, Y., Zhao, D., Guo, Q., 2018. Biosens. Bioelectron. 101, 123–128.
Noor bakhsh, A., Salimi, A., 2011. Biosens. Bioelectron. 30, 186–196.
Peng, L., Yuan, Y., Fu, X., Fu, A., Zhang, P., Chai, Y., Gan, X., Yuan, R., 2019. Anal. Chem. 91, 3239–3245.
Pyati, R., Richter, M.M., 2007. Phys. Chem. 103, 12–78.
Qiu, Y., Zhou, B., Yang, X., Long, D., Hao, Y., Yang, P., 2017. ACS Appl. Mater. Interfaces 9, 16848–16856.
Richter, M.M., 2004. Chem. Rev. 104, 3003–3036.
Sha, Y., Zhang, X., Li, W., Wu, W., Wang, S., Guo, Z., Zhou, J., Su, X., 2016. Talanta 147, 220–225.
Shahdost-fard, F., Salimi, A., Khezrian, S., 2014. Biosens. Bioelectron. 53, 355–362.
Shao, H., Lin, H., Lu, J., Hu, Y., Wang, S., Huang, Y., Guo, Z., 2018. Biosens. Bioelectron. 118, 247–252.
Shi, G.F., Cao, J.T., Zhang, J.J., Huang, K.J., Liu, Y.M., Chen, Y.H., Ren, S.W., 2014. Analyst 139, 5827–5834.
Shi, G.F., Cao, J.T., Zhang, J.J., Liu, Y.M., Chen, Y.H., Ren, S.W., 2015. Sens. Actuators, B 220, 340–346.
Subrahmanyam, S., Piletsky, S.A., Piletska, E.V., Chen, B., Karim, K., Turner, A.P.F., 2001. Biosens. Bioelectron. 16, 631–637.
Swanick, K.N., Ladouceur, S., Zysman-Colman, E., Ding, Z., 2012. Angew. Chem. Int. Ed. 51, 11079–11082.
Tang, Y., Zhang, S., Wen, Q., Huang, H., Yang, P., 2015. Anal. Chim. Acta 881, 148–154.
Teymourian, H., Salimi, A., Khezrian, S., 2017. Electroanalysis 29, 409–414.
Tian, D., Zhang, H., Chai, Y., Cui, H., 2011. Chem. Commun. 47, 4959–4961.
Vo-Dinh, T., Cullum, B., 2000. J. Anal. Chem. 366, 540–551.
Volinia, S., Galasso, M., Costinean, S., Tagliavini, L., Gamberoni, G., Drusco, A., Marchesini, J., Mascellani, N., Sana, M.E., Jarour, R.A., 2010. Genome Res. 20, 589–599.
Wang, S., Ge, L., Yan, M., Yu, J., Song, X., Ge, S., Huang, J., 2013. Sens. Actuators B Chem. 176, 1–8.
Wang, H., He, Y., Chai, Y., Yuan, R., 2014. Nanoscale 6, 10316–10322.
Wang, H., Yuan, Y., Chai, Y., Yuan, R., 2015. Small 11, 3703–3709.
Wang, T., Wang, D., Padelford, J.W., Jiang, J., Wang, G., 2016a. J. Am. Chem. Soc. 138, 6380–6383.
Wang, Y.L., Cao, J.T., Chen, Y.H., Liu, Y.M., 2016b. Anal. Methods 8, 5242–5247.
Wang, M., Zhou, Y., Yin, H., Jiang, W., Wang, H., Ai, S., 2018. Biosens. Bioelectron. 107, 34–39.
Wu, B., Wang, Z., Xue, Z., Zhou, X., Du, J., Liu, X., Lu, X., 2012. Analyst 137, 3644–3652.

Wulff, G., 2013. Microchim. Acta 180, 1359–1370.
Xie, C., Gao, S., Guo, Q., Xu, K., 2010. Microchim. Acta 169, 145–152.
Xie, S., Dong, Y., Yuan, Y., Chai, Y., Yuan, R., 2016. Anal. Chem. 88, 5218–5224.
Xiong, C., Liang, W., Wang, H., Zheng, Y., Zhuo, Y., Chai, Y., Yuan, R., 2016. Chem. Commun. 52, 5589–5592.
Yamato, H., Ohwa, M., Wemet, W., 1995. Anal. Chem. 67, 2776–2780.
Yang, B., Li, J., Zhang, L., Xu, G., 2016. Analyst 141, 5822–5828.
Yang, H.Y., Wang, H.J., Xiong, C.Y., Chai, Y.Q., Yuan, R., 2017a. ACS Appl. Mater. Interfaces 9, 36239–36246.
Yang, J.J., Cao, J.T., Wang, H., Liu, Y.M., Ren, S.W., 2017b. Talanta 167, 325–332.
Yang, L., Li, Y., Zhang, Y., Fan, D., Pang, X., Wei, Q., Du, B., 2017c. ACS Appl. Mater. Interfaces 9, 35260–35267.
Yue, H., Zhou, Y., Wang, P., Wang, X., Wang, Z., Wang, L., Fu, Z., 2016. Talanta 153, 401–406.
Zhang, N., Fu, X., Xu, Y.J., 2011. J. Mater. Chem. 21, 8152–8158.
Zhang, M., Ge, L., Ge, S., Yan, M., Yu, J., Huang, J., Liu, S., 2013. Biosens. Bioelectron. 41, 544–550.
Zhang, P., Wu, X., Yuan, R., Chai, Y., 2015. Anal. Chem. 87, 3202–3207.
Zhang, W., Xiong, H., Chen, M., Zhang, X., Wang, S., 2017. Biosens. Bioelectron. 96, 55–61.
Zhang, J., Shen, Y., Liu, Y., Hou, Z., Gu, Y., Zhao, W., 2018. Analyst 143, 4199–4205.
Zhao, J., Lei, Y.M., Chai, Y.Q., Yuan, R., Zhuo, Y., 2016. Biosens. Bioelectron. 86, 720–727.
Zhou, J., Liu, Z., Li, F., 2012. Chem. Soc. Rev. 41, 1323–1349.
Zhou, Y., Chen, S., Luo, X., Chai, Y., Yuan, R., 2018. Anal. Chem. 90, 10024–10030.
Zhu, W., Khan, M.S., Cao, W., Sun, X., Ma, H., Zhang, Y., Wei, Q., 2018. Biosens. Bioelectron. 99, 346–352.
Zhuo, Y., Wang, H.J., Lei, Y.M., Zhang, P., Liu, J.L., Chai, Y.Q., Yuan, R., 2018. Analyst 143, 3230–3248.
Zijlmans, H., Bonnet, J., Burton, J., Kardos, K., Vail, T., Niedbala, R.S., Tanke, H.J., 1999. Anal. Biochem. 267, 30–36.